LASER AND PLASMA SURFACE TREATMENTS OF PPS/CF
THERMOPLASTIC COMPOSITE LAMINATES FOR PRIMER ADHESION

A THESIS SUBMITTED TO
THE GRADUATE SCHOOL OF NATURAL AND APPLIED SCIENCES
OF
MIDDLE EAST TECHNICAL UNIVERSITY

BY

MERVE ATLIOĞLU

IN PARTIAL FULFILLMENT OF THE REQUIREMENTS
FOR
THE DEGREE OF MASTER OF SCIENCE
IN
METALLURGICAL AND MATERIALS ENGINEERING

APRIL 2023

Approval of the thesis:

LASER AND PLASMA SURFACE TREATMENTS OF PPS/CF THERMOPLASTIC COMPOSITE LAMINATES FOR PRIMER ADHESION

submitted by **MERVE ATLIOĞLU** in partial fulfillment of the requirements for the degree of **Master of Science** in **Metallurgical and Materials Engineering, Middle East Technical University** by,

Prof. Dr. Halil Kalıpçılar
Dean, Graduate School of **Natural and Applied Sciences**

Prof. Dr. Ali Kalkanlı
Head of the Department, **Metallurgical and Materials Eng.**

Prof. Dr. Cevdet Kaynak
Supervisor, **Metallurgical and Materials Eng., METU**

Examining Committee Members:

Prof. Dr. Necati Özkan
Polymer Science and Technology, METU

Prof. Dr. Cevdet Kaynak
Metallurgical and Materials Eng., METU

Assist. Prof. Dr. Ayşe Çağıl Kandemir
Mechanical Eng., TED University

Assist. Prof. Dr. Salih Ertan
Chemical Eng., Atılım University

Assist. Prof. Dr. Yusuf Keleştemur
Metallurgical and Materials Eng., METU

Date: 24.04.2023

I hereby declare that all information in this document has been obtained and presented in accordance with academic rules and ethical conduct. I also declare that, as required by these rules and conduct, I have fully cited and referenced all material and results that are not original to this work.

Name Last name : Merve Atlıoğlu

Signature :

ABSTRACT

LASER AND PLASMA SURFACE TREATMENTS OF PPS/CF THERMOPLASTIC COMPOSITE LAMINATES FOR PRIMER ADHESION

Atlıoğlu, Merve
Master of Science, Metallurgical and Materials Engineering
Supervisor: Prof. Dr. Cevdet Kaynak

April 2023, 87 pages

After production and characterization of Poly(phenylene sulfide) / Carbon Fiber (PPS/CF), thermoplastic composite laminates, the main purpose of this study was, to evaluate effects of "laser" and atmospheric "plasma" surface treatments on the adhesion performance of primer painting by comparing with "untreated" and traditional "sandblasted" samples.

For this purpose, after surface characterization of untreated and treated samples by Wettability, SEM, XPS, FT-IR analyses; adhesion characteristics of an industrial primer paint applied onto the surfaces were evaluated by using two different industrial methods: "Cross-cut Adhesion" tests and "Three-point Bending Adhesion" tests.

Compared to the Untreated samples, it was observed that all surface treated samples could be assigned with the "best" primer adhesion grade of GT0, and having at least two times more maximum "Separation Load" with "cohesive" separation mechanism of primer paint layers.

The success of the Sandblasted samples could be attributed to the increased micro-level surface roughness, while for the Laser treated samples nano-level surface

roughness, both of them leading to decreased Contact Angle values, and increased Total Surface Free Energy values. The success of the Plasma treated samples could be attributed to the increased number of chemically reactive sites formed by the oxidation of carbon and sulphur elements in PPS matrix.

ÖZ

ASTAR TUTUNMASI İÇİN PPS/CF TERMOPLASTİK KOMPOZİT LAMİNATLARIN LAZER VE PLAZMA YÜZEY İŞLEMLERİ

Atlıoğlu, Merve
Yüksek Lisans, Metalurji ve Malzeme Mühendisliği
Tez Yöneticisi: Prof. Dr. Cevdet Kaynak

Nisan 2023, 87 sayfa

Poli(fenilen sülfit) / Karbon Elyaf (PPS/CF) termoplastik kompozit laminatların üretimi ve karakterizasyonundan sonra, bu çalışmanın temel amacı, "lazer" ve atmosferik "plazma" yüzey işlemlerinin astar boya yapışma performansı üzerindeki etkilerini "işlenmemiş" ve geleneksel "kumlanmış" numunelerle karşılaştırarak değerlendirmektir.

Bu amaçla, işlem görmüş ve işlem görmemiş numunelerin Islanabilirlik, SEM, XPS, FT-IR analizleri ile yüzey karakterizasyonu yapıldıktan sonra; yüzeylere uygulanan bir endüstriyel astar boyanın yapışma özellikleri, "Cross-cut Yapışma" testleri ve "Üç-nokta Eğme Yapışma" testleri olmak üzere iki farklı endüstriyel yöntem kullanılarak değerlendirilmiştir.

İşlenmemiş numunelerle karşılaştırıldığında, tüm yüzey işlemli numunelerin "en iyi" astar yapışma derecesi olan GT0 sınıfı ve astar boya katmanlarının "kohezyonlu" ayırma mekanizması ile en az iki kat daha fazla maksimum "Ayırma Yükü" elde edebileceği görülmüştür.

Kumlanmış numunelerin başarısı mikro düzeyde artan yüzey pürüzlülüğüne, Lazerle işlenmiş numunelerin başarısı için ise nano seviyede artan yüzey pürüzlülüğü ile elde edilen Temas Açısı değerlerinin azalmasına ve Toplam Yüzey Serbest Enerji

değerlerinin artmasına, bağlanabilir. Plazma ile işlenmiş numunelerin başarısı ise, PPS matrisindeki karbon ve kükürt elementlerinin oksidasyonu ile oluşan kimyasal olarak reaktif bölgelerin artan sayısına bağlanabilir.

Anahtar Kelimeler: Poli(fenilen sülfür) (PPS), Karbon Elyaf (CF), Astar Boyama, Yüzey İşlemleri, Kumlama, Lazer İşlemi, Plazma İşlemi

To my niece, Melinda.

ACKNOWLEDGMENTS

TABLE OF CONTENTS

LIST OF TABLES

LIST OF FIGURES

FIGURES

NOMENCLATURE

ASTM	American Society for Testing and Materials
Cp	Specific Heat Capacity
CFRP	Carbon Fiber Reinforced Polymer
DoC	Degree of Crystallinity
DMA	Dynamic Mechanical Analysis
DSC	Differential Scanning Calorimetry
IPA	Isopropyl alcohol
ISO	International Organization for Standardization
Nd:YAG	Neodymium-doped Yttrium Aluminum Garnet
SD	Standard Deviation
SBS	Short Beam Strength
Tg	Glass-transition Temperature
θ	Contact Angle
γ_{LV}^{D}	Dispersion Components of Liquid Surface Tension
γ_{LV}^{P}	Polar Components of Liquid Surface Tension
γ_{SV}	Total Surface Free Energy
γ_{SV}^{D}	Dispersion Components of Surface Free Energy
γ_{SV}^{P}	Polar Components of Surface Free Energy

CHAPTER 1

INTRODUCTION

Many industries including aeronautical manufacturers have been using light weight polymer matrix composites reinforced with continuous fibers having superior stiffness and strength required for structural parts. Today, there are many efforts to replace traditional thermoset matrices of continuous fiber reinforced composites with thermoplastic matrices. Because, thermoset matrix composites have disadvantages of brittle behaviour, long production cycles, irreversible formation, recycling difficulty, and limited storage time. Therefore, use of high-performance thermoplastic polymers, such as poly(etheretherketone) (PEEK), poly(etherketoneketone) (PEKK), poly(aryletherketone) (PAEK), and poly(phenylenesulfide) (PPS) as the matrix material is on the rise. Apart from glass fibers and aramid fibers, the most widely used continuous fiber reinforcement in these thermoplastic matrices are carbon fibers. In this thesis, the thermoplastic composite system used was poly(phenylenesulfide) (PPS) matrix reinforced with continuous woven carbon fibers (CF).

1.1   PPS/CF Thermoplastic Composite Laminates

PPS macromolecules are made up of an aromatic ring connected to a sulfide atom (Figure 1.1). Compared to conventional thermoplastics, PPS has higher mechanical, and thermal properties. For instance, it has tensile strength and modulus of 85 MPa and 4.2 GPa; while its typical glass transition temperature, melting temperature and degradation temperatures are 85°C, 290°C and 530°C, respectively. Moreover, its semi-crystallinity degree could be nearly 40% [1–6].
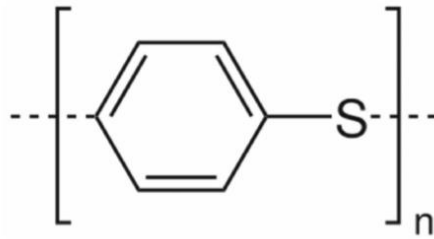
Figure 1.1 Monomer structure of PPS.

PPS/CF composites have certain applications in a variety of industries, including aerospace, automotive, electronics and electrical [7]. Depending on the structural requirement, PPS matrix could be combined with different forms of carbon fiber. For instance, chopped fibers are frequently used in automotive industry, while continuous fibers are preferred for the structural parts in aerospace industry.

In the market, PPS/CF are available in the form of preimpregnated continuous fibers known as "prepregs". During production of PPS/CF parts, prepreg layers are stacked one upon another using a consolidation process to obtain the composite laminate structure with desired properties. The most widely used consolidation processes for thermoplastic composite laminates are compression moulding and autoclave moulding; in which thermoplastic matrix melts at high temperatures and solidifies by cooling under pressure, taking the shape of the mold.

1.2   Painting of Composite Structures

Painting is a crucial process for aerospace parts in terms of their surface protection, maintenance, operation, performance and appearance. Composite structures especially outer components can be very susceptible to environmental degradation. Paints could extend the life of these composite structures by acting as a barrier to environmental degradation effects of sunlight, rain, moisture and bacteria. Painting also provides a smooth surface to inspect cracks and other damages. If they exist,

paint can be removed for the repairment, and then reapplied. Moreover, smooth and well-applied paint can help to improve the aerodynamics of an aircraft by reducing the air drag and decreasing the fuel consumption.

Paints are generally applied as two layers; the first one named as "primer-coat" while the second one "top-coat" in order to achieve ultimate protection. The satisfactory performance of these two paint coatings throughout the service life of an aircraft part depends on many aspects. Painting composite structures requires specialized techniques and materials, as regular paints cannot adhere properly to the smooth surfaces of composite parts. A typical painting process includes the following steps:

(i) *Paint Preparation*

First of all, viscous paint base (primer or top-coat) must be thoroughly stirred or shaken in order to disperse pigments and other additives they may contain. Then, other chemicals (e.g. hardeners, thinners) should be mixed with the base paint in a specific order. Paint mixtures might also need an induction time, a minimum period after mixing, so that spray painting would be proper. Paint mixtures have limited pot life after mixing.

(ii) *Surface Preparation*

Before primer-paint application, surface cleaning would be necessary to remove the surface dirt and contaminants by using certain solvents such as isopropanol (IPA), methyl–ethyl–ketone (MEK) and acetone. After the solvent cleaning, composite surfaces should be treated further to achieve intermolecular interactions and mechanical interlocking between the surface and the paint; which will be discussed in Section 1.4.

(iii) *Primer Application*

Primers are the first thin (15–25 µm) organic coating layers applied to the cleaned and treated composite surfaces. Due to the presence of active corrosion inhibitors, their primary function is to serve as a physical barrier against environmental and chemical degradation. Another function is to enhance adhesion of the top-coat to the composite part surface. Figure 1.2 (a) shows primer painting of an aircraft by a spray mechanism.

(iv) *Top-Coat Application*

Top-coats are the second and rather thick (60–120 µm) organic coating layers applied to the primer coated composite surfaces. Top-coats should be applied over primers within the recommended recoating time interval. Their main function is also to protect the composite parts from environmental attacks by acting as a barrier. Top-coat painting is also very crucial for cosmetic purposes. Figure 1.2 (b) shows top-coat paint application over primer painted aircraft.

(v) *Drying and Curing*

Drying and curing operations required for many thermoset based primer and top-coat applied parts are done in an environment controlled paint shops. At room temperature, these operations might take place for 7 days or more. In order to decrease time, warm air in drying chambers or infrared heating could be used.

Figure 1.2 Images of an aircraft, after (a) primer painting and (b) top-coat painting.

1.3   Primer and Top-Coat Paints Used for Aircraft Composite Parts

In the aerospace industry, selection of the paint type depends on the stringent environmental requirements such as exposure to extreme temperatures, harsh atmospheric conditions, UV radiation, fire resistance and toxicity standards. Primer and top-coat paint systems used for the composite aircraft parts could be classified into two main groups; (i) epoxy-based paints, and (ii) polyurethane-based paints.

Epoxy based systems are especially used for interior parts, including fuel tanks due to mainly their high corrosion protection performance; while polyurethane-based systems are generally preferred for exterior parts (such as fuselage, wing, tail) because of their high environmental resistance properties.

Epoxy based paint systems are two-component systems; the base component being an epoxy resin mixed with pigments, corrosion inhibitors, extenders, additives, and solvents. The second component is the hardener or curing solution containing the curing agent (amine or polyamide) and a solvent. Polyurethane based paint systems mainly form by a reaction between the primary and secondary hydroxyl groups of the polyol (polyester or acrylate resin) and aliphatic isocyanates resulting in urethane crosslinks [8]. In this study, one of the epoxy-based primer paint system is used.

1.4 Surface Treatments Before Primer Application

Since surface energies of the thermoplastic aromatic polymer matrices are low, it is difficult for the primer paint to wet their surfaces. Therefore, in order to have certain degree of primer adhesion, a kind of surface treatment must be applied to eliminate surface impurities and to enhance wettability by mechanical or chemical techniques.

For the thermoplastic matrix composite parts, available methods used in the aircraft industry can be divided in two groups; "traditional mechanical techniques" (such as grinding and sandblasting) and "chemical energetic techniques" (such as laser and plasma).

(i) *Grinding and Sandblasting*

Aircraft industry has traditionally utilized mechanical abrasion methods with abrasive-grain sandpapers to polish the surface, get rid of contaminants, and change the surface roughness profile. When the grit size is increased, surface roughness increases proportionally, but with fiber damages.

Sandblasting is a further abrasion method applied, in which stream of mineral or metallic particles are aggressively accelerated to the material to activate its surface. Sandblasting results in surfaces with irregular topography and roughness. Similar to grinding, it also causes fiber damages on the composite surface.

6

Thus, these traditional techniques cannot eliminate human mistakes or inconsistencies. They could harm the bulk composite and fibers on the surfaces by causing delamination flaws. Moreover, they produce a lot of dust, which, if trapped under the primer paint layer, have the potential to contaminate surfaces leading to poor adhesion.

Therefore, in order to promote adhesion between the primer paint and the thermoplastic matrix composite surfaces, chemical energetic surface treatment methods (such as laser and plasma) are preferred. In this study, both of them are used.

(ii) *Laser Surface Treatment*

Laser surface treatment is a non-contact, environmentally friendly method that is simple to control and automate. By optimizing the laser parameters (e.g. power, wavelength, pulse distance) the surface chemistry and the roughness could be tailored precisely. In order to prevent human error and inconsistent surface characteristics, laser treatment processes can ensure high reliability and repeatability for aerospace structural components [9]. Figure 1.3 schematically compares effects of traditional and laser treated composite surface with reinforcing fibers. It should be noted that laser treatment also leads to "fiber stripping", i.e. matrix removal from the fibers located at the surface, which enhances the interlocking action at the interface to improve adhesion [10].
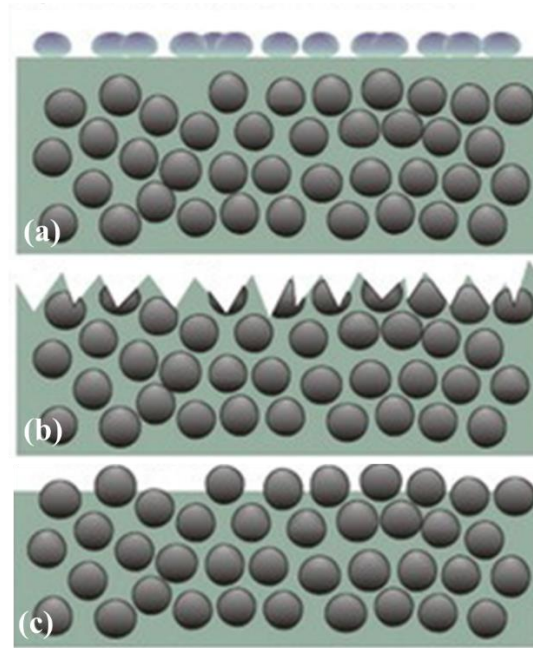
Figure 1.3 Schematic of (a) Contaminated surface, (b) Grinded/sandblasted surface, and (c) Laser treated surface [11].

Laser ablation is the process of surface modification by material removal. Ablation occurs when the target material absorbs energy from laser irradiation such that the energy of its atoms or ions becomes higher than their binding energy. Laser pulse duration and intensity together with material properties determine the degree of material removal from the surface [12].

As shown in Figure 1.4, photoionization is the first step on a laser-induced material surface. During photoionization, valence electrons absorb enough energy from incident laser photons to move to the conduction band. In this band, free electrons are generated by multiphoton ionization or by impact ionization. At increased kinetic energies, subsequent collisions of energized free electrons result in the emission of secondary electrons through inverse bremsstrahlung absorption. This leads to an avalanche growth in the number of free electrons and, finally, material removal through melting or vaporization [12].
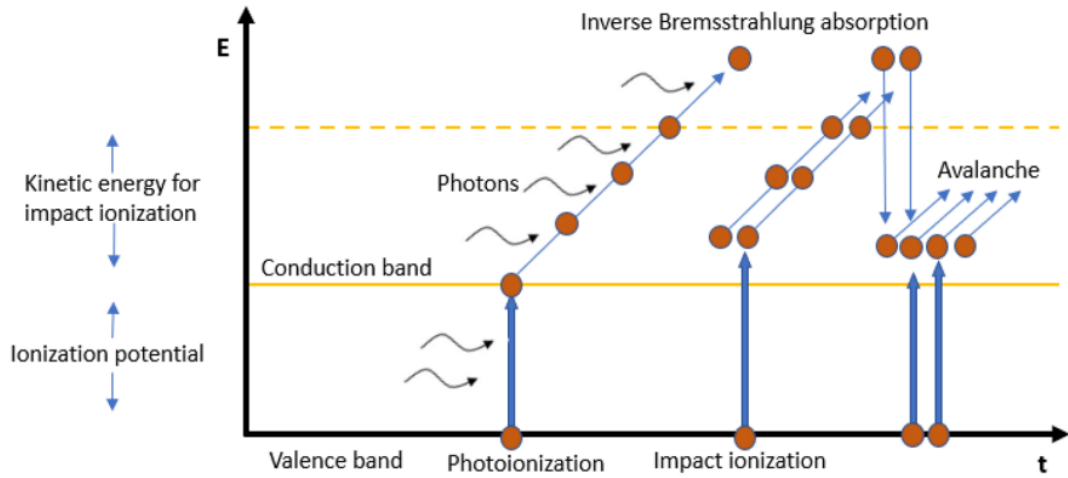
Figure 1.4 Steps of photoionization, inverse bremsstrahlung and impact ionization during laser treatment [12].

Several types of lasers are used in the industry for different purposes such as cutting, drilling, marking, creating patterns, cleaning and improving adhesion. Use of Nd:YAG laser (i.e. Neodymium-doped Yttrium Aluminum Garnet (Nd:$Y_3Al_5O_{12}$)) is rather new in laser ablation surface treatment method. Nd: YAG lasers commonly produce infrared light with a wavelength of 1064 nm. However, the high intensity pulses can be effectively frequency doubled to produce laser light at 532 nm or at higher harmonics of 355 and 266 nm by employing crystals made of optically non-linear materials. Both continuous and pulsed operations are possible with Nd:YAG lasers. The normal mode of operation for Nd:YAG lasers is Q-switching [13].

As illustrated in Figure 1.5, during treatment, sample substrate is placed on a two-axis moveable stage and the laser beam is kept stationary. Scanning parameters such as scan speed, scan width and pulse distance are controlled by the stage software. The beam expander is mostly used to vary the focus spot size of a focusing lens to maintain the beam collimation in systems with long beam paths.
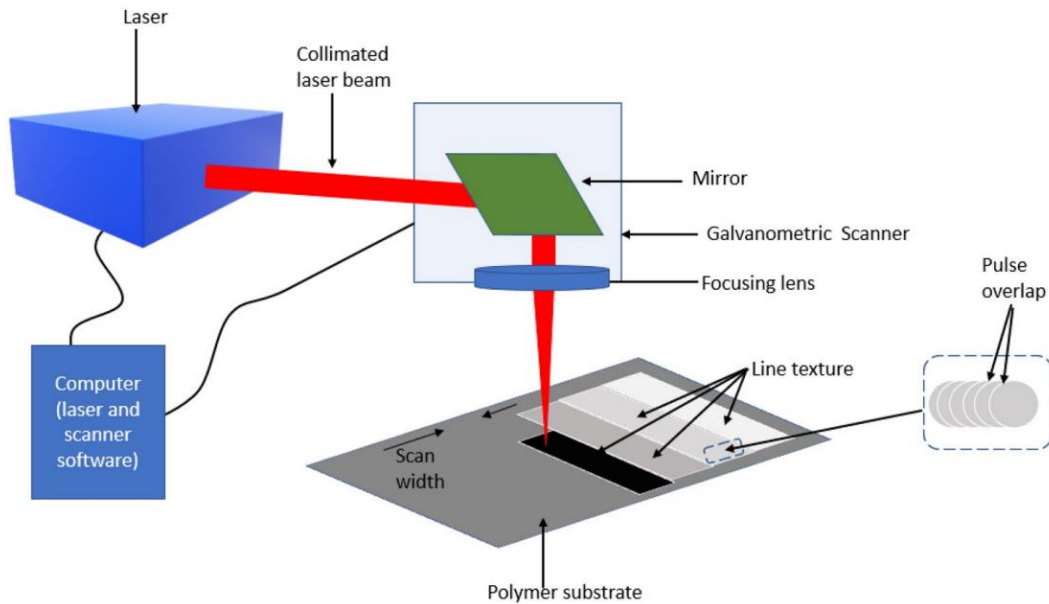
Figure 1.5 Typical laser surface treatment system [12].

(iii) *Plasma Surface Treatment*

Plasma surface treatments are used for many polymer surfaces due to leading significant degree of surface activation required in many coating processes including painting [14]. Unlike the "low-pressure plasma" alternative, atmospheric pressure plasma systems, simply named as "atmospheric plasma", provide in-line process capabilities, low prices, and minimal environmental and human safety requirements [15].

Plasma is a gas of charged and neutral particles containing cations and electrons. Atmospheric plasma systems (Figure 1.6) create consistent, high-density mixture of ions, electrons, and free radicals using a capacitive discharge at atmospheric pressure. The charged particles then direct these reactive species onto the surface, where the charged particles activate or react [16, 17]. When the surface of the substrate is exposed to plasma, multiple reactions between reactive molecules and radicals can lead to the formation of a film.
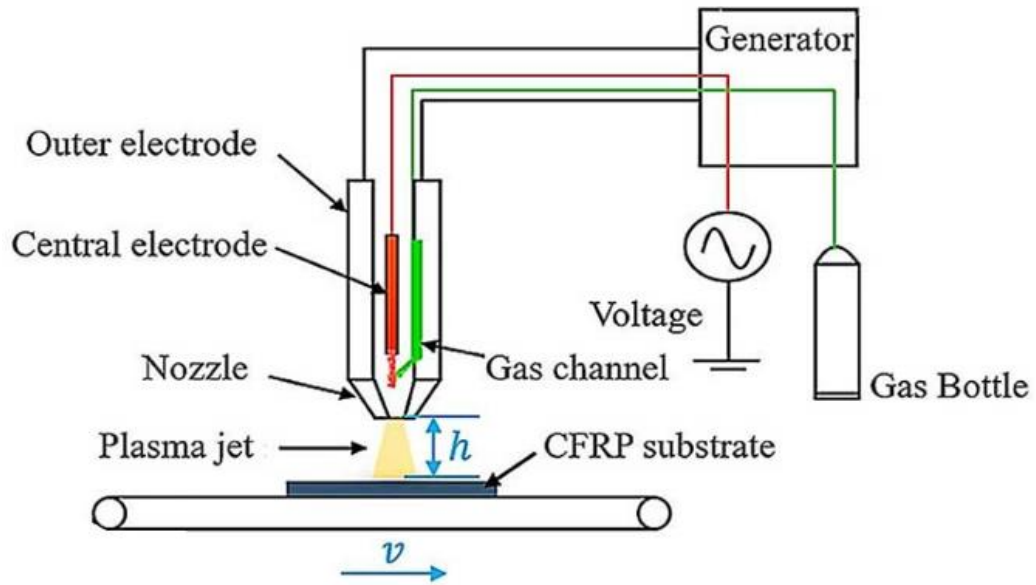
Figure 1.6 Typical atmospheric plasma surface treatment system.

Lu *et al.* [18] indicated that during low-pressure plasma surface treatment of PEEK/CF thermoplastic composite substrate, generation of reactive surface groups C–O, C=O and O–C=O take place via the proposed oxidation mechanisms illustrated in Figure 1.7.
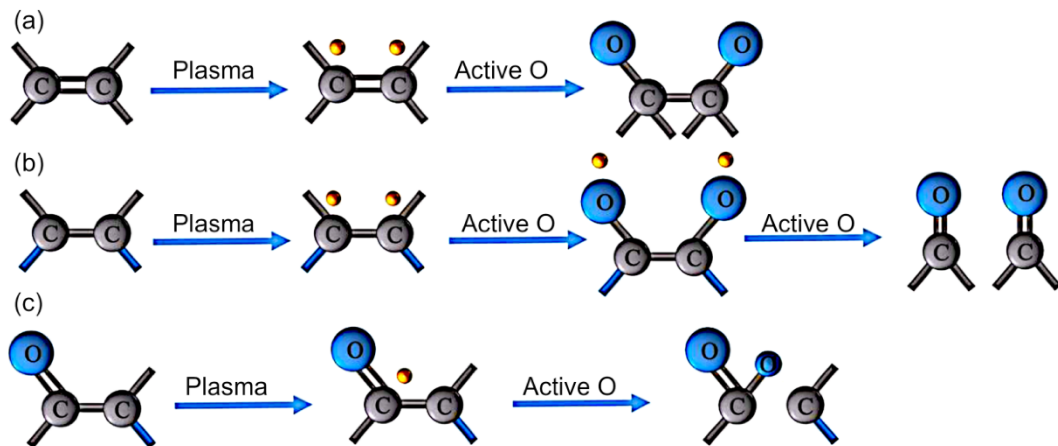
Figure 1.7 Proposed oxidation mechanisms for the generation of: (a) C–O, (b) C=O bonds, and (c) O–C=O reactive groups during plasma treatment of PEEK/CF composite surface [18].

For the PPS/CF composite surface; in addition to O–C=O functional groups, sulfone O=S=O and carboxyl sulfoxide S=O functional groups could be formed during plasma surface treatments, as illustrated by Xu *et al.* [19] in Figure 1.8. These groups lead to promotion of cohesion by way of inducing chemical reactions or generating hydrogen bond with components of the primer paint [19].
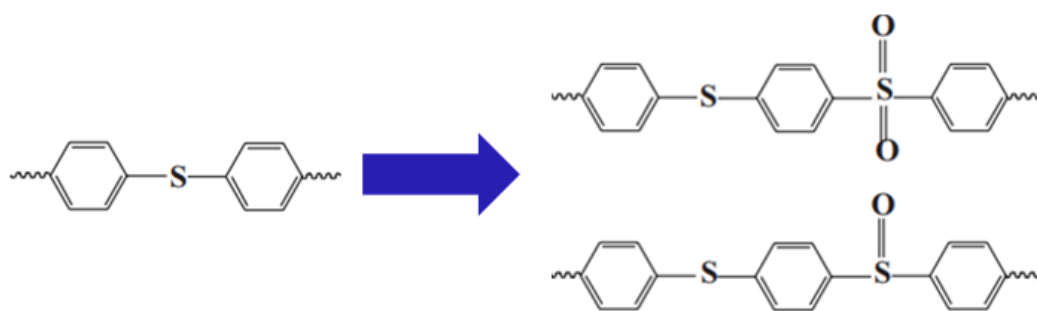
Figure 1.8 Formation of O=S=O and S=O functional groups during plasma surface treatment of PPS/CF composite substrate [19].

1.5   Evaluation of Primer Adhesion
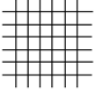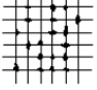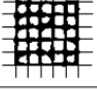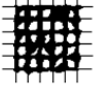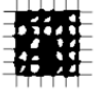
It is known that effects of surface treatment methods (sandblasting, laser, plasma, etc.) on the surfaces of polymer matrix composites could be characterized by Contact Angle measurements, SEM, XPS and FT-IR analyses. On the other hand, to evaluate primer adhesion performance, there are very limited number of techniques being mostly qualitative. In the industry, the following two standardized tests are used. Therefore, these tests are also preferred in this study.

(i) *Cross-cut Adhesion Test*

The cross-cut adhesion test (ISO 2409 standard) is a qualitative approach to evaluate the resistance of paint coatings to separation from substrates when a right-angle

lattice pattern is cut into the coating, penetrating through the substrate. By using a multi-blade cutting tool, six parallel cuts are formed in two directions making a lattice pattern (Figure 1.9). After removing any loose paint from the area of cutting and a very careful visual examination of the lattice pattern is made. Then, the appearance of the lattice pattern is compared with the classification table given by the standard (Table 1.1). Depending on the degree of paint flaking from the cross-cut lattice pattern, paint adhesion is classified into six classes, as GT0, GT1, GT2, GT3, GT4, GT5, from the best to the worst.

Table 1.1 Classification of paint adhesion according to ISO 2409 Cross-cut test standard.

Classification	Description	Appearance of surface of cross-cut area from which flaking has occurred[a] (Example for six parallel cuts)
0	The edges of the cuts are completely smooth; none of the squares of the lattice is detached.	
1	Detachment of small flakes of the coating at the inter-sections of the cuts. A cross-cut area not greater than 5 % is affected.	
2	The coating has flaked along the edges and/or at the intersections of the cuts. A cross-cut area greater than 5 %, but not greater than 15 %, is affected.	
3	The coating has flaked along the edges of the cuts partly or wholly in large ribbons, and/or it has flaked partly or wholly on different parts of the squares. A cross-cut area greater than 15 %, but not greater than 35 %, is affected.	
4	The coating has flaked along the edges of the cuts in large ribbons and/or some squares have detached partly or wholly. A cross-cut area greater than 35 %, but not greater than 65 %, is affected.	
5	Any degree of flaking that cannot even be classified by classification 4.	—

[a] The figures are examples for a cross-cut within each step of the classification. The percentages stated are based on the visual impression given by the pictures and the same percentages will not necessarily be reproduced with digital imaging.
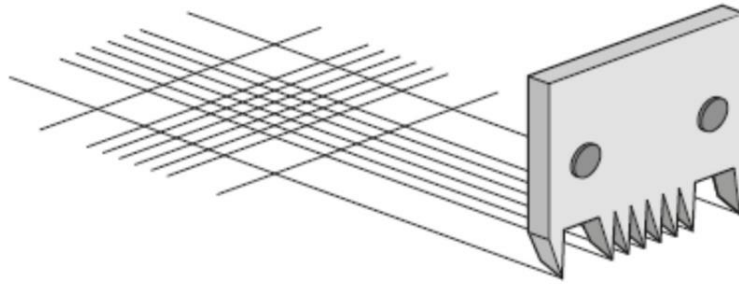
Figure 1.9 Creation of the lattice pattern by a multi-blade cutting-tool during cross-cut paint adhesion test.

(ii) *Three-point Bending Adhesion Test*

The three-point bending adhesion test (ISO 14679 standard) is rather a quantitative approach to evaluate adhesion characteristics of paint systems (primer and top-coat) applied on a rigid substrate (such as metals and composite laminates). First, as shown in Figure 1.10, at the center of the painted composite laminate specimen, a thermosetting rigid block is moulded, then three-point bending load is applied to the whole system until failure. The maximum load recorded in the load-displacement curve is defined as "adhesion power" of the interface between the composite laminate and the paint layer.
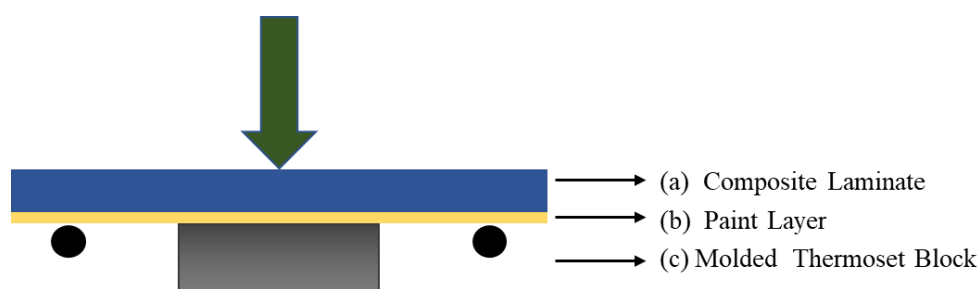
Figure 1.10 Specimen configuration of three-point bending adhesion test used for painted composite laminates.

1.6   Literature Review

Literature review on the use of "Laser and Plasma Surface Treatments" for Thermoplastic Matrix Composites revealed that, these studies [14, 20–30] were mainly concentrated on the improvement of bonding and joining processes. There was no reported study on the use of Laser Treatments to improve primer paint or top-coat paint adhesion, while there were extremely limited number of studies, being only two [31, 32], on the use of Plasma Treatments for the Improvement of Primer Adhesion, as summarized below.

Bres *et al.* [31] applied atmospheric-pressure plasma treatment to increase polymer surface reactivity for strong and long-term paint adhesion on poly(etheretherketone)/ carbon fiber (PEEK/CF) composite surfaces. Two operational parameters "scanning speed" (0.3 m/s) and "distance between the nozzle and surface" (27 mm) was kept constant, while changing the "power" parameter for both "air" and "nitrogen" plasma. Treated surfaces were characterized by contact angle wettability measurement, XPS chemical analysis, and AFM topography analyses. Adhesion performance of the paint was characterized by cross-cut adhesion and three-point bending adhesion tests. They indicated that both air and nitrogen plasma treatments improved the paint adhesion to the industrially acceptable high grades of GT0 and GT1 according to cross-cut tests. Maximum load measurements during three-point bending adhesion tests revealed that use of air plasma resulted in top-surface degradation due to oxidation, while use of nitrogen plasma resulted in better paint adherence basically due to surface nano roughness modification.

Lapena *et al.* [32] studied paint adhesion performance on the carbon fiber reinforced polyaryl ether ketone (PAEK/CF) composite substrate by applying atmospheric pressure "Ar-O_2" plasma surface treatment. Water contact angle and XPS analyses were performed to characterize treated surfaces, while cross-cut and three-point bending tests were conducted for paint adhesion. They indicated that use of only cross-cut tests were not appropriate since untreated surfaces also passed the paint

adhesion performance with high grades of GT0 and GT1. Then, measurements by three-point bending adhesion tests revealed that Ar-O_2 plasma treated surfaces had much higher primer and top-coat paint adherence, basically due to the increased levels of the oxygen and nitrogen polar groups. They also concluded that adherence performance of top-coat paint alone (without primer layer) was very high.

1.7   Aim of the Thesis

It was observed that, in the literature, although there are other PPS/CF related studies [14, 20–30] investigating various aspects of thermal behavior, mechanical properties, production and joining of PPS/CF composite structures, no studies were reported on the use of laser or plasma surface treatments to improve primer and top-coat paint adhesion.

Therefore, after production and characterization of the PPS/CF thermoplastic composite laminates, the main purpose of this study was, as the first time in the literature, to evaluate effects of both "laser" and atmospheric "plasma" surface treatments on the adhesion performance of primer painting. Their adhesion performance was also compared with respect to the "untreated" and traditional "sandblasted" samples.

For this purpose, after surface characterization of untreated and treated samples by Wettability, SEM, XPS, FTIR analyses; adhesion characteristics of an industrial primer paint applied onto the surfaces were evaluated by using two different industrial methods: "Cross-cut Adhesion" tests and "Three-point Bending Adhesion" tests.

CHAPTER 2

EXPERIMENTAL WORK

Experimental work conducted in this study was basically composed of a "preliminary step" and then the "main step". In the preliminary step, polyphenylene sulfide (PPS)/ carbon fiber (CF) thermoplastic composite laminates were produced, as explained in Section 2.1 below. In order to characterize these laminates, various analyses and tests were conducted, and the results are given in Appendices A, B, C. Then, as the main step, effects of both laser and plasma surface treatments were evaluated in terms of primer paint adhesion applied to the laminate surfaces, as explained in Sections 2.2 through 2.5.

2.1   Production of PPS/CF Composite Laminates

PPS/CF thermoplastic composite laminates were produced first by supplying their commercially available prepregs, and then consolidating them process via compression molding method.

(i)   *PPS/CF Prepregs Supplied*

Tradename of the supplied PPS/CF prepregs with the thickness of 0.31 mm was *Toray-TenCate Cetex® TC1100*. Their matrix was a semi-crystalline PPS engineering thermoplastic having glass transition temperature (T_g), melting temperature (T_m), and processing temperature (T_p) range of 90°C, 280°C, and 300–330°C, respectively. In these prepregs, PPS matrix was reinforced with woven CF forms having 5-harness satin (5HS) weave style, as illustrated in Figure 2.1.
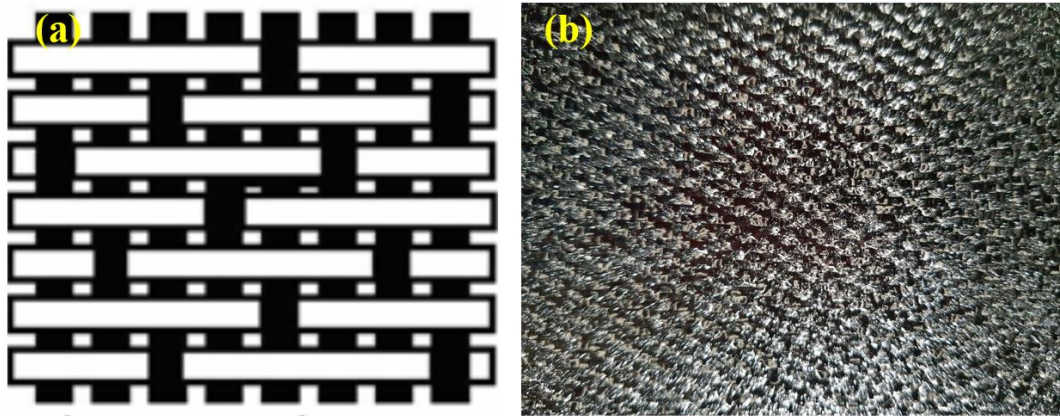
Figure 2.1 (a) Schematic of 5-harness satin weave style, and (b) PPS/CF prepreg supplied.

(ii) *Consolidation of PPS/CF Prepregs*

PPS/CF composite laminates were produced by consolidation of certain number of prepreg layers via compression molding technique. In this method, first prepregs were cut into 55 x 200 mm by using an automated ply cutter. In order to get 2 mm thick laminates, 7 plies were stacked on a mold surface having a polyimide (*Kapton*) release film. Consolidation above the melting temperature of PPS matrix was achieved by using a hot-pressing system (*Langzauner Perfect)* as shown in Figure 2.2; while the heating, pressing and cooling steps applied were as follows:

- Increase the press force to 350 kN and the temperature to 315°C, and hold for 30 min.
- Increase the press force to 550 kN, and hold for 10 min.
- Cool down to room temperature with 5°C/min ramp.

Figure 2.2 Production of PPS/CF laminates; (a) Prepreg lay-up, (b) Consolidation by compression molding, and (c) A laminate produced.

2.2 Surface Treatments Applied Before Primer Painting

It is known that to improve primer paint adhesion on the surfaces of polymer matrix composite laminates, energetic surface treatments such as "laser" and "plasma" could be applied to form chemically active surface functional groups. In this study both of them were used. Moreover, since in the industry, the traditional "sandblasting" method has been still used; effects of laser and plasma treatments would be also compared with the influences of sandblasting.

Before any of these surface treatments, PPS/CF laminates produced were first cut into 100 x 150 mm by using a diamond tip industrial cutter (*Diamond-3, 3515RS*) with a cooling unit. After cutting, all surfaces were cleaned to get rid of residues by using a solvent (*Isopropyl Alcohol, IPA*). Thus in this study, laminates investigated and compared could be grouped into four conditions: "untreated", "sandblasted", "laser treated", and "plasma treated". These surface treatments applied are summarized below.

(i) *Sandblasting*

In this traditional method laminate surfaces were sandblasted by using alumina sand particles having average size of 177 µm via a blasting jet gun equipment (8 mm nozzle diameter, 2.5 bar air pressure) at 100 mm distance, 45°-60° projection angle for about 60 seconds. After sandblasting, laminates were rinsed properly with DI water, and then dried in a furnace at 60°C for 2 hours. These steps are shown in Figure 2.3.
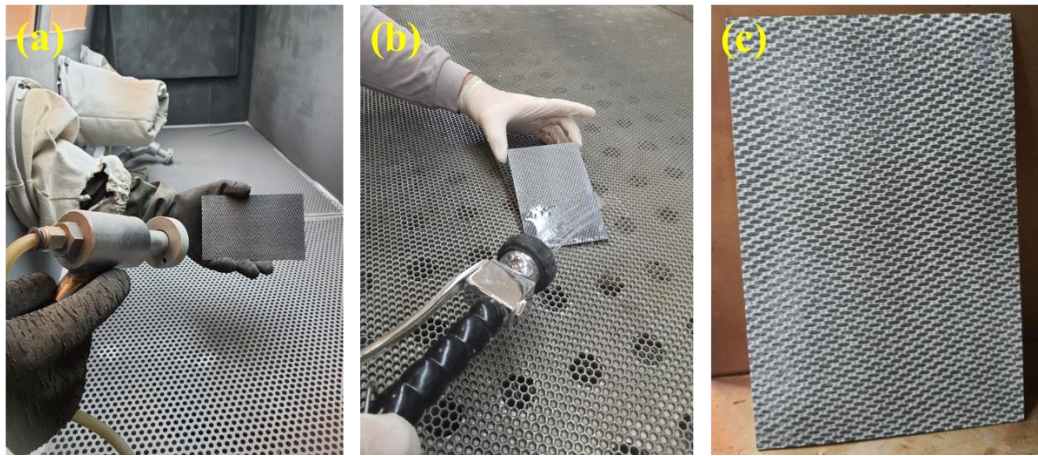
Figure 2.3 Sandblasting surface treatment method; (a) Blasting with alumina sand, (b) Rinsing with DI water and (c) Drying in a furnace.

(ii) *Laser Treatment*

Laser treatment of the laminate surfaces was conducted by using the laboratory scale Q-switched Nd-YAG laser set-up (*Teknofil, Coherent*) generating 266 nm wavelength. Laminates were placed on an X-Y axis controlled table robot (*Aerotech, ALS3600*); while the laser head was hold steady. The system is shown in Figure 2.4.

In order to reveal effects of laser surface treatment, it was possible to use four different operational parameters of the system by adjusting different values. In this study, the following four parameters with their different values were investigated.

- Laser Power (mW): 100, 140, 170, 200, 230
- Laser Scanning Speed (mm/s): 30, 40, 50
- Laser Pulse Distance (μm): 100, 200
- Laser Focal Distance (mm): 9, 10, 11
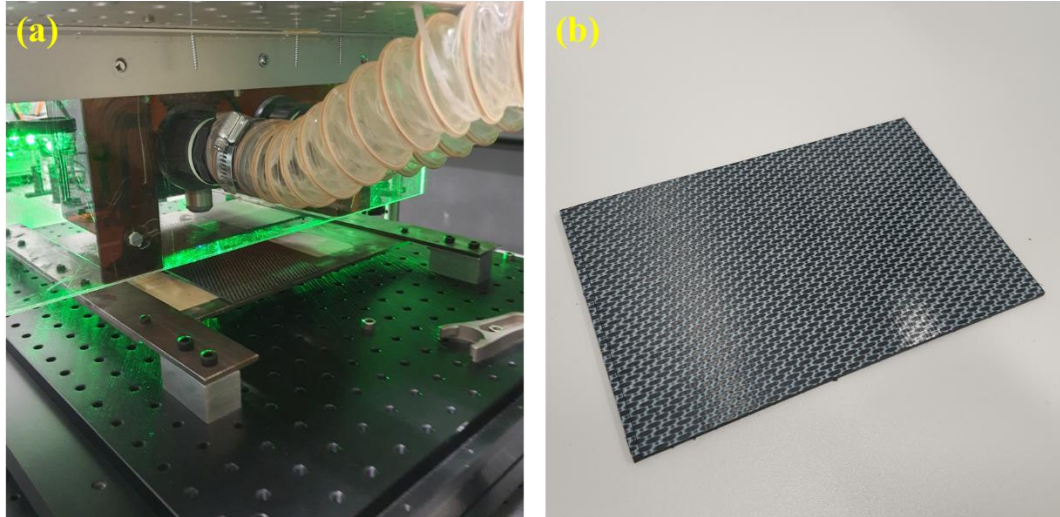
Figure 2.4 (a) Laser surface treatment system, and (b) An example of the laser-treated laminate surface.

(iii) *Plasma Treatment*

In this study, plasma treatment of the laminate surfaces was conducted by using a laboratory scale system (*Plasmatreat, RD2004*) which could operate at atmospheric pressure, therefore treatments done under these systems was also called as "Atmospheric Plasma Treatment". As shown in Figure 2.5, the system has a rotating plasma jet nozzle that could be controlled by an X-Y-Z axis table robot (*HKTM, Toyo*).

The plasma medium used was "air" plasma. Following two different operational parameters with their different values were evaluated in order to observe their possible different influences.

- Plasma Scanning Speed (mm/s): 5, 20, 100, 150
- Plasma Nozzle Distance (mm): 6, 12, 24
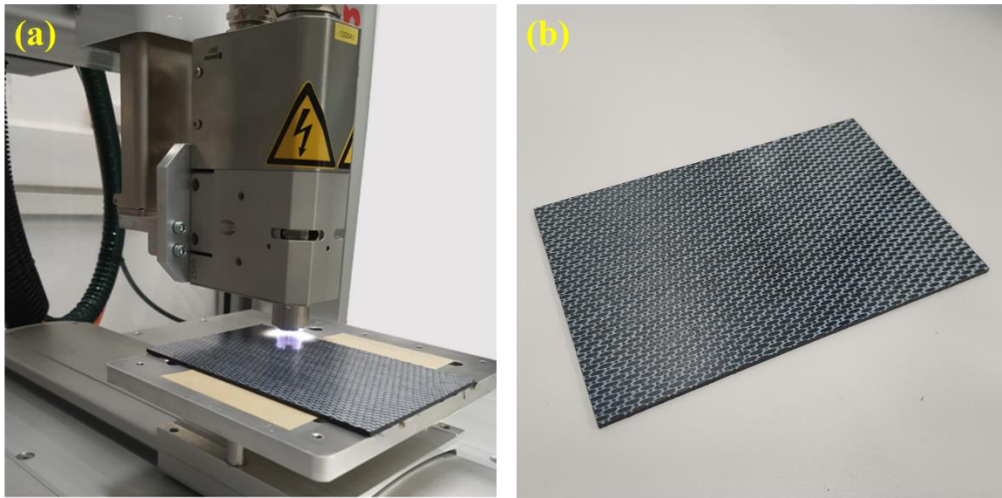
Figure 2.5 (a) Atmospheric plasma surface treatment system and (b) An example of the plasma-treated laminate surface.

2.3 Characterization of the Treated Surfaces Before Primer Painting

In order to characterize untreated, sandblasted, laser and plasma treated PPS/CF laminate surfaces, the following four analyses were conducted.

(i) *Contact Angle Measurement and Surface Energy Estimation*

Contact angle measurements of untreated and all treated surfaces were achieved by using an optical tensiometer (*Biolin Scientific, Attention Theta Lite*) (Figure 2.6 (a)).

First, PPS/CF laminates were placed on the sample platform for high-resolution camera images. Then, sessile drops of 4-5 μl deionized water was placed on the laminate surface. "Water Contact Angles" were measured from the images taken by the camera.

The main objective of contact angle measurement was to estimate "Surface Free Energy" of untreated, sandblasted, laser and plasma treated PPS/CF surfaces in accordance with ASTM D5725 standard. Total surface free energy and its polar and dispersion components were estimated by using the Owens-Wendt-Rabel-Kaelble (OWRK) equation [30, 33] given below;

$$(1 + \cos\theta)\gamma_{LV} = 2[(\gamma_{SV}^D \gamma_{LV}^D)^{\frac{1}{2}} + (\gamma_{SV}^P \gamma_{LV}^P)^{\frac{1}{2}}]$$

In this equation, θ is the measured contact angle of liquid with the solid surface, γ_{LV} is the total surface tension of the liquid, while γ_{LV}^D and γ_{LV}^P are its "dispersion" and "polar" components, respectively. The total surface tension of the polar and dispersion components of "deionized water" and "formamide" is known. Therefore, in order to estimate total surface free energy (SFE), i.e. γ_{SV} of the untreated and treated PPS/CF solid surfaces, all contact angle measurement were repeated by using this time sessile drops of "formamide". Then, it was possible to determine total surface free energy γ_{SV} of the samples by adding its polar (γ_{SV}^P) and dispersion (γ_{SV}^D) components as;

SFE of PPS/CF samples = $\gamma_{SV} = \gamma_{SV}^P + \gamma_{SV}^D$

(ii) *Scanning Electron Microscopy (SEM)*

Surface morphology of the treated laminate surfaces was observed under a field emission scanning electron microscope (Zeiss, Sigma 300 SEM) (Figure 2.6 (b)) at an accelerating voltage of 5 kV. Since PPS/CF samples have certain level of conductivity, no gold sputtering was necessary.

(iii) *X-ray Photoelectron Spectroscopy (XPS)*

Chemical composition of the treated laminate surfaces was investigated by X-ray photoelectron spectroscopy (*Thermo Fisher Scientific, K-Alpha*) (Figure 2.6 (c)). For the emission of photoelectrons with element-specific binding energies, surfaces were scanned under monochromatic Al-Kα radiation (1486.7 eV).

(iv) *Fourier-transform Infrared Spectroscopy (FT-IR)*

Fourier-transform infrared spectroscopy (*Perkin Elmer, Spectrum One)* was used in order to reveal formation of functional groups on the surfaces of treated laminate samples (Figure 2.6 (d)). At least 32 scans were signal-averaged by the diamond attenuated total reflectance (Di-ATR) unit of the spectrometer in the wavenumber range of 650-4000 cm^{-1} with a resolution of 4 cm^{-1}.

2.4   Primer Painting of Treated Surfaces

In this study, the primer paint system used was a three-component epoxy based commercial primer (*Akzo Nobel, Aerodur Barrier Primer 37045*), compatible with a wide range of composites and polymers. It is stated that, this white-coloured primer has low water permeability with high resistance to aircraft hydraulic fluids and other chemicals.

Main steps used during primer application onto the surface treated PPS/CF laminate samples are illustrated in Figure 2.7. First, in order to disperse all pigments present in the base primer uniformly, it was stirred in a shaker. Then, 50 parts hardener was added to the 100 parts base epoxy, and stirred again thoroughly. For the required level of viscosity, 100-125 parts thinner was added eventually.
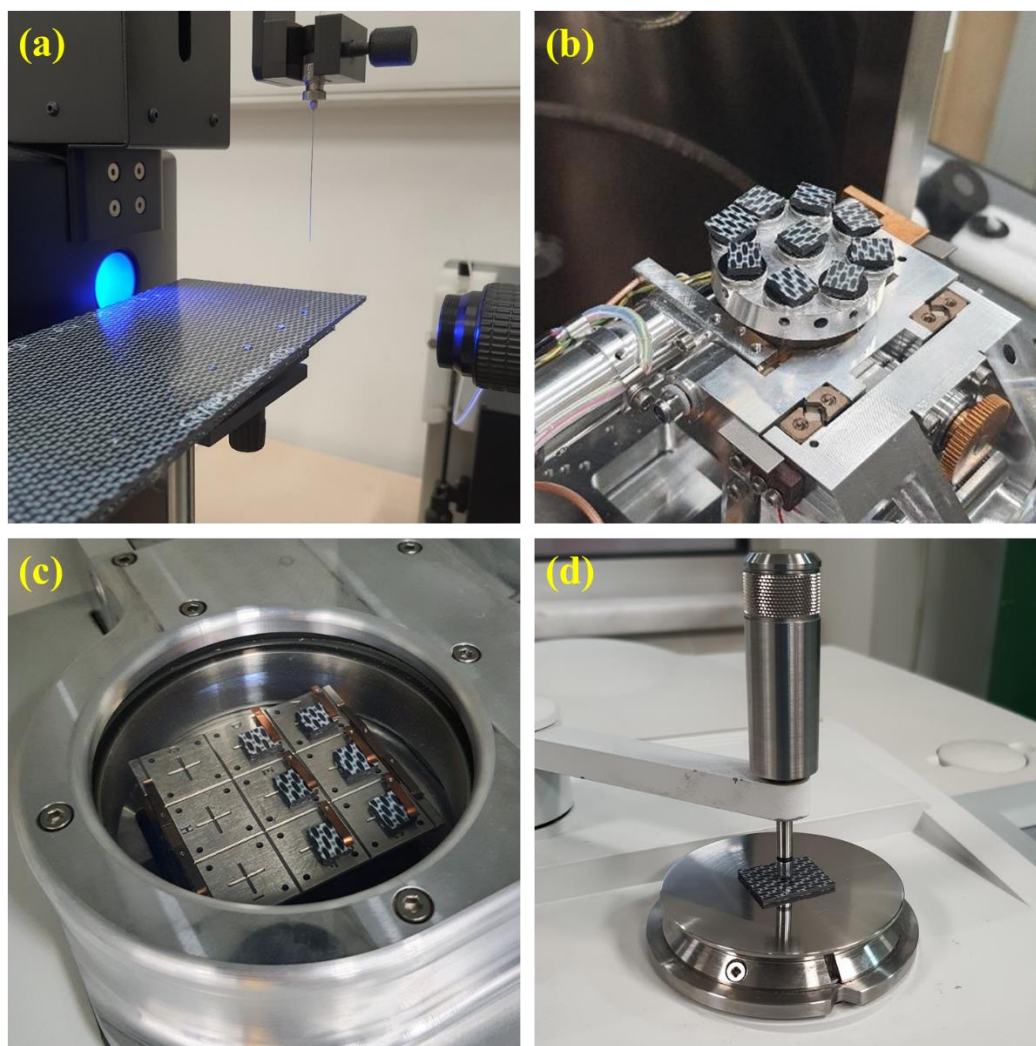
Figure 2.6 Characterization of the surface treated laminate samples: (a) Contact angle measurement, (b) SEM, (c) XPS, and (d) ATR-FTIR.

Primer mixture was applied onto the treated laminate surfaces by using a spray gun mechanism, successively; so that the approximate primer thickness would be 20 µm. After primer spraying, laminate samples were cured/dried in a room at 60° for 2 hours.
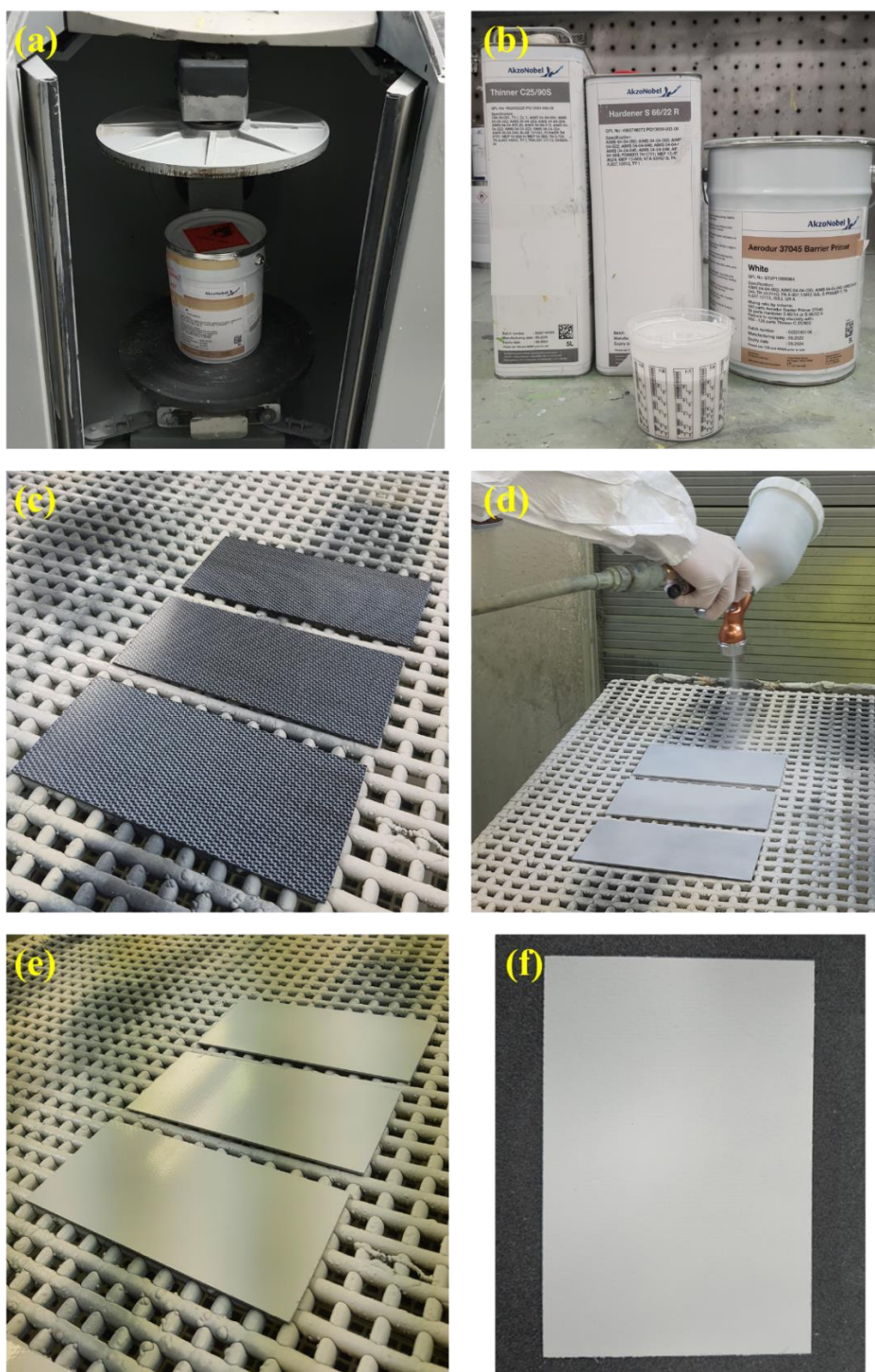
Figure 2.7 Primer painting of surface treated PPS/CF laminate samples: (a) Stirring the base epoxy primer, (b) Mixing the base primer with hardener and thinner, (c) Surface treated laminates before primer application, (d) Primer painting by a spray gun mechanism, (e) Curing/drying after primer application, and (f) An example of primer painted laminate sample.

26

2.5   Testing for Adhesion Performance of Primer Paint

In this study, in order to evaluate effects of all surface treatments on the primer paint adhesion performance; two different standardized industrial testing techniques were used: "cross-cut" and "three-point bending" adhesion tests.

It should be noted that, in the industry, primer and top-coat paint adhesion tests were conducted usually in two different conditions; the first one being just after the painting operations, while the second one is after immersing the painted specimens in water for a certain period. According to ISO-2812 standard, painted specimens should be immersed in de-ionized water for 7 or 14 days. Therefore, in this study all primer adhesion performance tests were conducted "before" and "after" 7 days water immersion.

(i) *Cross-cut Adhesion Test*

This test is a qualitative approach to evaluate the resistance of primer paint against separation from composite laminate surface, when a right-angle lattice pattern was cut into the primer layer. As shown in Figure 2.8, by using a hand-held multi-blade cross-cutting device (*Elcometer 1542, 6 teeth, 1 mm*), six parallel cuts were formed in two directions making a lattice pattern in accordance to ISO-2409 standard.
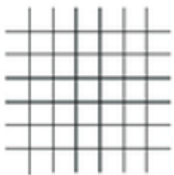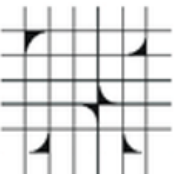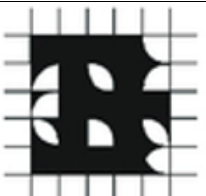
Then, primer paint residues were cleaned from the area of cutting by using a brush and also an adherent tape. Under a magnifier, the appearance of the lattice pattern was inspected carefully, and then compared with grade classification table given by the standard (Table 2.1). Finally, depending on the degree of primer paint flaking from the cross-cut lattice pattern, primer adhesion performance was graded as GT0, GT1, GT2, GT3, GT4, GT5; in which industrially acceptable adhesion grades are only GT0 and GT1.
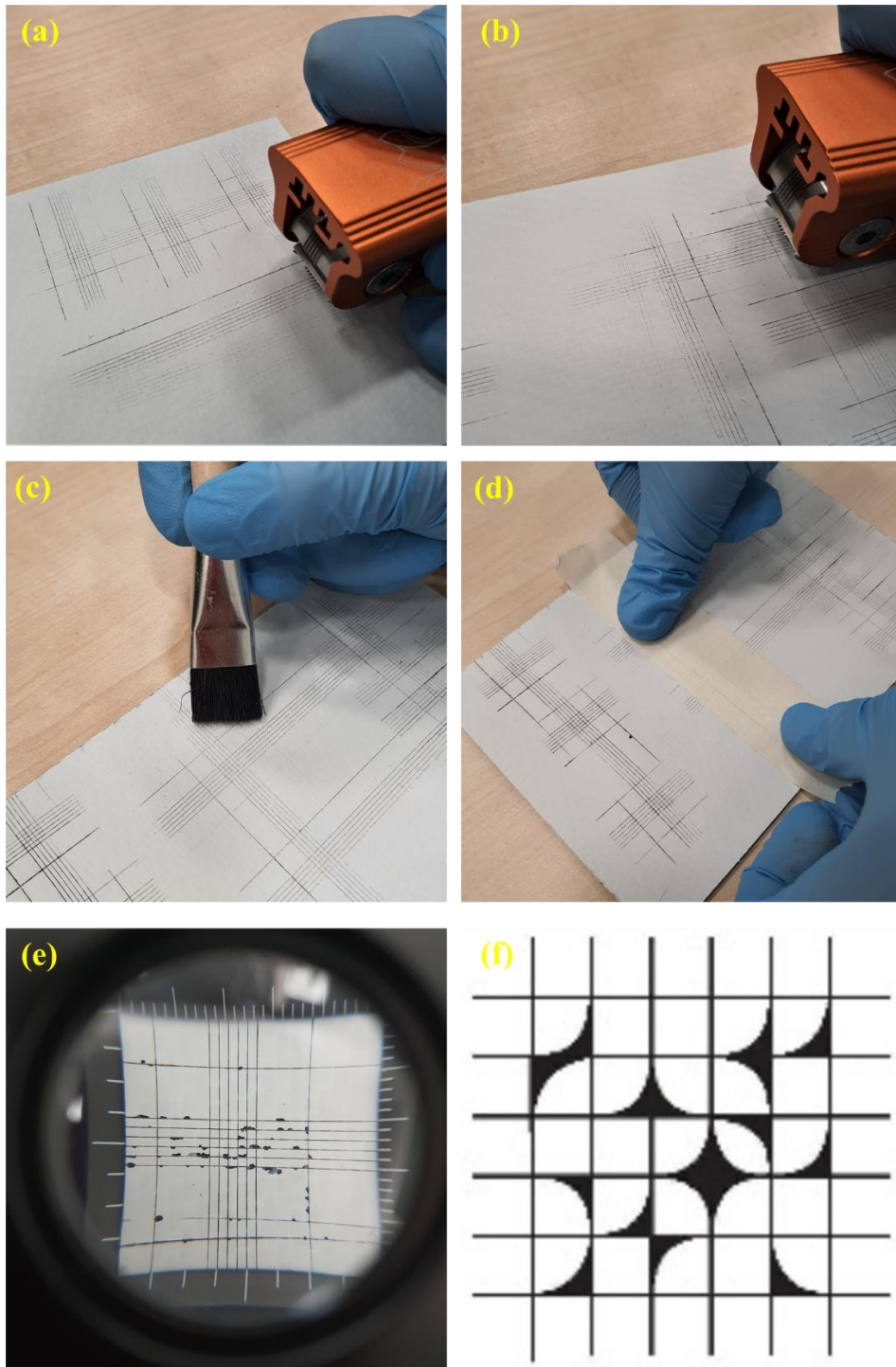
Figure 2.8 Cross-cut primer adhesion test: (a) and (b) Formation of cross-cut lattice pattern by vertical and horizontal cutting, (c) and (d) Cleaning of the primer residues from the cutting area by brushing and adherent tape removing, (e) and (f) Inspection of the lattice pattern under a magnifier, and comparing the appearance with the ones given in the standard table.

Table 2.1 Grade classification of the primer paint adhesion performances according to ISO-2409 Cross-cut test standard.

Adhesion Grade	Appearance of the Lattice to Compare	Percent Area Flaked	Description
GT0		0	None of the squares of the lattice is detached.
GT1		<5%	Detachment of small flakes of the primer paint at the intersections of the cuts.
GT2		5-15%	Primer paint has flaked along the edges and/or the intersection of the cuts.
GT3		15-35%	The coating has flaked along the edges of the cuts partly or wholly in large ribbons, and/or it has flaked partly or wholly on different parts of the squares.
GT4		35-65%	Primer paint has flaked along the edges of the cuts in large ribbons and/or some squares have detached partly or wholly.
GT5	-	>65%	Any degree of flaking that cannot even be classified by classification 4.

(ii) *Three-point Bending Adhesion Test*

Compared to cross-cut test, that test is rather a quantitative approach to evaluate the resistance of primer paint against separation from the composite laminate surface under three-point loading. As shown in Figure 2.9, first on the center of the 2 x10 x 50 mm primer painted laminate specimen, a thermosetting (Loctite EA 934NA AERO) rigid block of 4 x 5 x 25 mm was molded in accordance with ISO 14679 standard.

Then, the whole specimen was three-point bending loaded by using a 10 kN Universal Testing System (*Instron 68TM*) with a span length of 33 mm. After separation of the primer paint layer together with the rigid block at the center, primer adhesion performance was evaluated first by visual inspection of the surfaces, and then quantitively by recording the maximum load reached in the load-deflection curve.
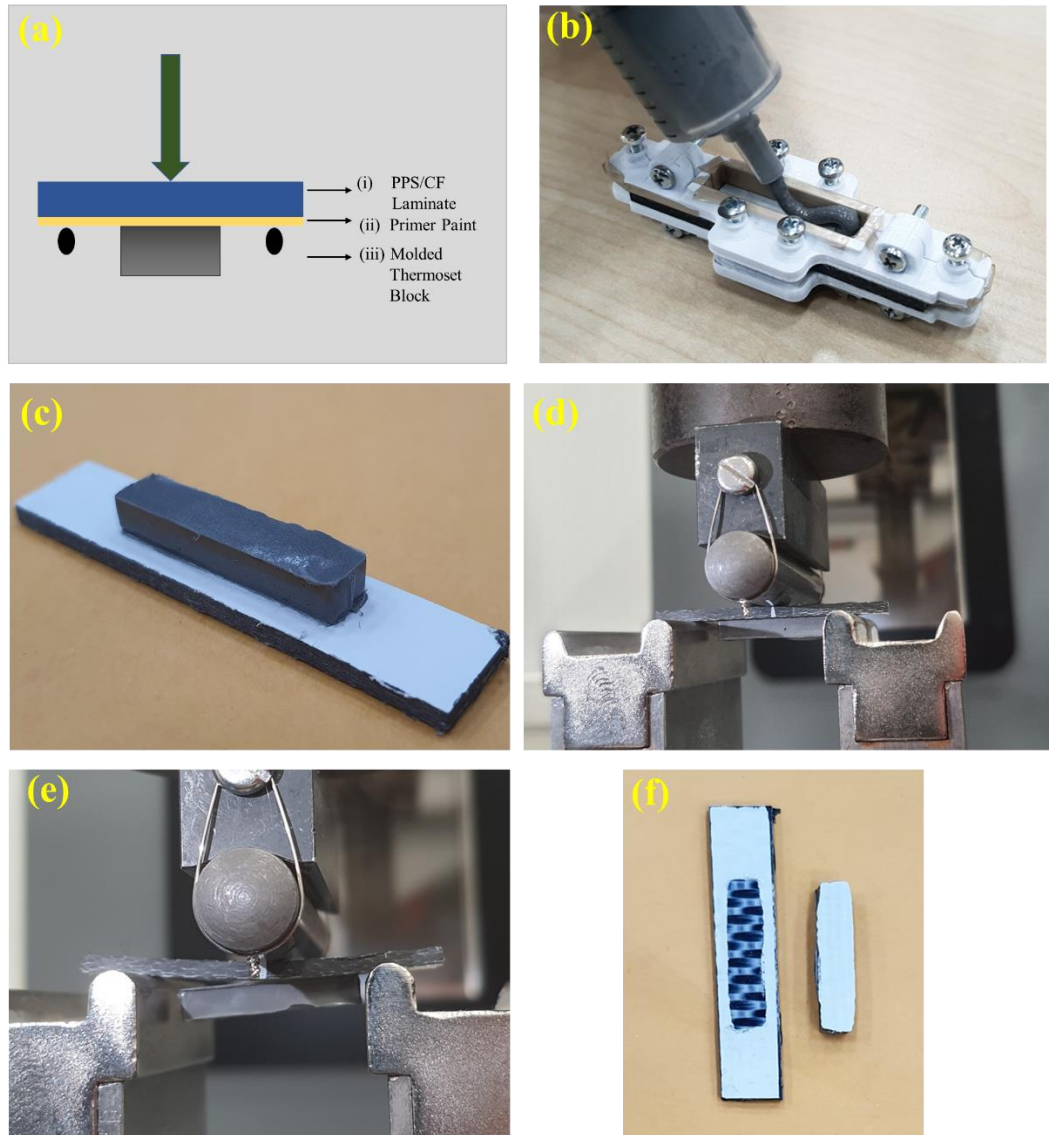
Figure 2.9 Three-point bending primer adhesion test: (a) Specimen configuration used, (b) Molding of thermosetting rigid block on the center of primer painted surface, (c) The whole specimen to be loaded, (d) Three-point bending loading during the test, (e) Separation of the primer paint layer together with the rigid block, and (f) Inspection of the separated interface.

CHAPTER 3

RESULTS AND DISCUSSION

The main purpose of this study was to investigate effects of two different surface treatments, i.e. laser and plasma, on the adhesion characteristics of an industrial primer paint applied onto the surfaces of PPS/CF thermoplastic composite laminates. Therefore, in this chapter, first in Section 3.1 preliminary surface treatment trials to determine process parameters were explained. Then in Section 3.2, effects of these surface treatments on the chemical and morphological characteristics of the surfaces were discussed. Finally, in Section 3.3, influences of treatments on the primer paint adhesion performance were elaborated.

3.1 Trials for the Laser and Plasma Surface Treatment Parameters

In the laser surface treatment equipment used, it was possible to change "four" processing parameters. Therefore, in order to observe influences of these four parameters, several different combinations were tried. For instance; for the "Laser Power" parameter values of 100, 140, 170, 200 mW, for the "Laser Scanning Speed" parameter values of 30, 40, 50 mm/s, for the "Laser Pulse Distance" parameter values of 100, 200 μm, for the "Laser Focal Distance" parameter values of 9, 10, 11 mm were used. Thus, the total number of trials having different combinations of the parameters were 48.

In the atmospheric plasma surface treatment equipment used, it was possible to change "two" processing parameters. Therefore, in order to observe influences of these two parameters, different combinations were tried. For example; for the "Plasma Scanning Speed" parameter values of 5, 20, 100, 150 mm/s, and for the "Plasma Nozzle Distance" parameter values of 6, 12, 24 mm were used. Thus, the total number of trials having different combinations of the parameters were 12.

Then, in order to choose three different process parameter combinations for each surface treatment method, "contact angle" measurements and "surface free energy" estimations were conducted for the 48 different laser treatment trials and 12 different plasma treatment trials. Results of all these trials were given in Appendix D, where values of Contact Angles (θ) and total Surface Free Energy (γ_{SV}) including its Polar (γ_{LV}^{P}) and Dispersion (γ_{LV}^{D}) components were tabulated in Table D.1 for the 48 different laser treated PPS/CF samples, and in Table D.2 for the 12 different plasma treated PPS/CF samples.

It is known that for the sufficient primer paint adhesion on the composite laminate surfaces, it is preferable to have "lower contact angle" and "higher surface energy" values. Therefore, the first elimination of the trials were done from this perspective.

Moreover, it is also known that surface treatments should not lead to severe physical damages on the composite laminate surfaces, such as "complete matrix removal", "fiber stripping", and "fiber damage". Thus, the second elimination of the trials were done by examining the treated surfaces under scanning electron microscope (SEM).

Then, all further analyses and tests were conducted for only these three process parameter combinations of laser and plasma surface treated PPS/CF samples, designed as Laser-1, Laser-2, Laser-3 and Plasma-1, Plasma-2, Plasma-3. For each treatment selected process parameter combinations are given in Table 3.1.

Table 3.1 Three different process parameter combinations selected for the Laser and Plasma surface treatment of PPS/CF samples.

	Laser Power (mW)	Scanning Speed (mm/s)	Pulse Distance (µm)	Focal Distance (mm)
Laser-1	140	30	100	9
Laser-2	170	30	100	9
Laser-3	170	40	100	9

	Scanning Speed (mm/s)	Nozzle to Surface Distance (mm)
Plasma-1	20	6
Plasma-2	150	6
Plasma-3	100	12

3.2   Effects of Treatments on the Surface Characteristics of the Samples

In order to observe effects of laser and plasma treatments on the various chemical and physical characteristics of the PPS/CF laminate surfaces, four different analyses (Contact Angle-Surface Energy, SEM, XPS, FT-IR) were conducted for "Laser-1, Laser-2, Laser-3" and "Plasma-1, Plasma-2, Plasma-3) samples one by one. It should be noted that, each analysis was also conducted for the "untreated" and the traditional "sandblasted" samples for comparative purposes.

3.2.1   Wettability Analyses of the Untreated and Treated Surfaces

It is known that "wettability" is a significant pre-requirement for the adhesion of a liquid medium (such as primer paint) on the solid surfaces (such as PPS/CF laminate). In this study, wettability analyses were conducted by Contact Angle

Measurements and Surface Free Energy Estimations for all samples. Measurements were repeated at least on three different locations of each specimen surface. Average values (with ± standard deviations) of "Water Contact Angle" and "Total Surface Free Energy" including its "Polar" and "Dispersion" components are tabulated in Table 3.2 and presented in Figure 3.1, respectively.

Table 3.2 Average values of the Water Contact Angle and Total Surface Free Energy including its Polar and Dispersion Components of Untreated and Treated PPS/CF surfaces.

	θ Water Contact Angle (°)	γ_{SV} Total Surface Free Energy (mJ/m^2)	γ_{SV}^{P} Polar Component (mJ/m^2)	γ_{SV}^{D} Dispersion Component (mJ/m^2)
Untreated	66.28 ± 0.84	35.48 ± 0.53	18.07 ± 0.68	19.11 ± 0.16
Sandblasted	87.32 ± 3.49	39.04 ± 0.05	1.65 ± 0.93	37.39 ± 0.99
Laser-1	55.20 ± 2.11	49.24 ± 1.14	19.06 ± 1.58	30.18 ± 0.44
Laser-2	57.24 ± 0.34	49.34 ± 0.16	16.45 ± 0.24	32.89 ± 0.07
Laser-3	55.43 ± 3.42	49.28 ± 1.81	18.70 ± 2.54	30.60 ± 0.72
Plasma-1	23.33 ± 2.34	69.61 ± 0.86	33.74 ± 1.12	35.87 ± 0.26
Plasma-2	27.72 ± 1.99	67.22 ± 0.85	32.61 ± 1.10	34.62 ± 0.25
Plasma-3	24.45 ± 0.80	68.92 ± 0.31	33.68 ± 0.40	35.23 ± 0.09

For the spontaneous wetting condition, it is known that a decreasing trend in the Contact Angle values play an important role. As shown in Table 3.2 and Figure 3.1, Contact Angle values of Untreated sample increased from 66° to 87° in the Sandblasted sample. On the other hand, in the Laser and Plasma treated samples, significant decreases were observed; for example in Laser-1 treated sample the angle decreased to 55°, for the Plasma-1 treated sample it was as low as 23°.
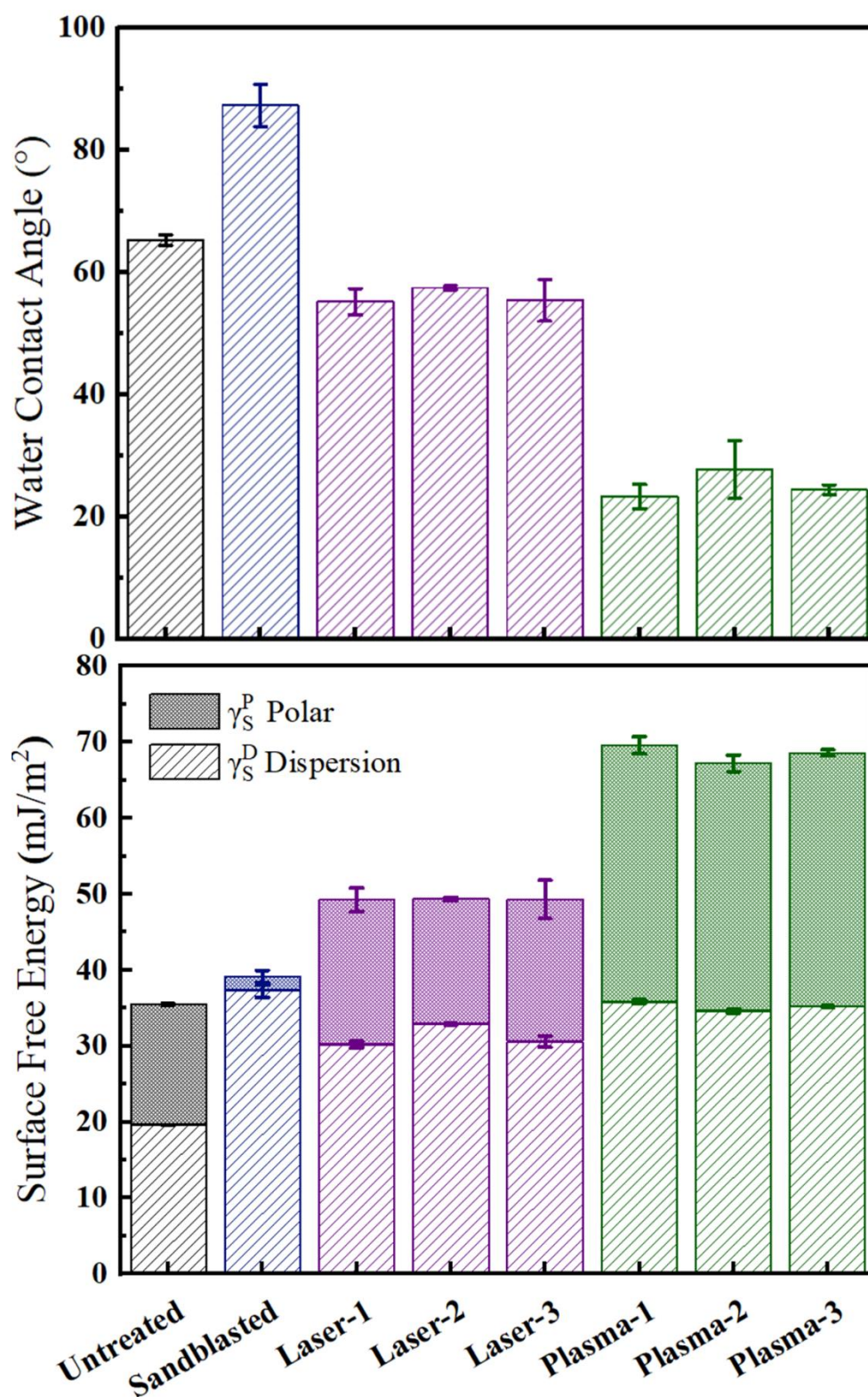
Figure 3.1 Water Contact Angle and Total Surface Free Energy including its Polar and Dispersion Components of Untreated and Treated PPS/CF surfaces.

Apart from importance of lower Contact Angle values, Surface Free Energy values of the solid surfaces should be as much as higher for efficient wetting and adhesion of the liquid medium. Table 3.2 and Figure 3.1 indicated that total Surface Free Energy of the Untreated sample slightly increased from 37 mJ/m^2 to 39 mJ/m^2 for the Sandblasted sample. For the Laser and Plasma treated samples increases were more significant. For instance, the increases were up to 49 mJ/m^2 for the Laser-1 and as much as 69 mJ/m^2 for the Plasma-1 treated samples.

It was also known that [14, 30, 34], the degree of "Polar Component" in the total Surface Free Energy values act as a driving force for the wettability and more significantly for the intermolecular chemical interactions leading to improved adhesion on the solid surfaces. It was seen that Polar Component of the Untreated sample was 18 mJ/m^2, which almost diminished in the Sandblasted sample. No significant changes were observed in the Laser treated samples; on the other hand, increases for the plasma treated samples were as much as up to 33 mJ/m^2.

3.2.2   SEM Analyses of the Untreated and Treated Surfaces

Since surface morphology of the composite laminates also influences primer paint adhesion, SEM analyses were conducted on different locations of all sample surfaces. Figure 3.2 displays examples of 500X magnification SEM images taken from the Untreated and Treated PPS/CF surfaces. Compared to the morphology of Untreated surface, it was seen that after all laser and plasma treatments, no significant changes were observed in terms of surface smoothness degree.

Contrarily, it was very apparent that, there was an enormous increase in the surface roughness of the Sandblasted sample surface with certain degree of "fiber stripping" and "fiber damage". However, this traditional mechanical surface treatment method has been still used before primer painting operations of composite aircraft parts. Because, the increased micro level surface roughness also increases effective surface area for wetting and enable mechanical interlocking at the interface, improving the adhesion between the composite laminate surface and the primer paint.
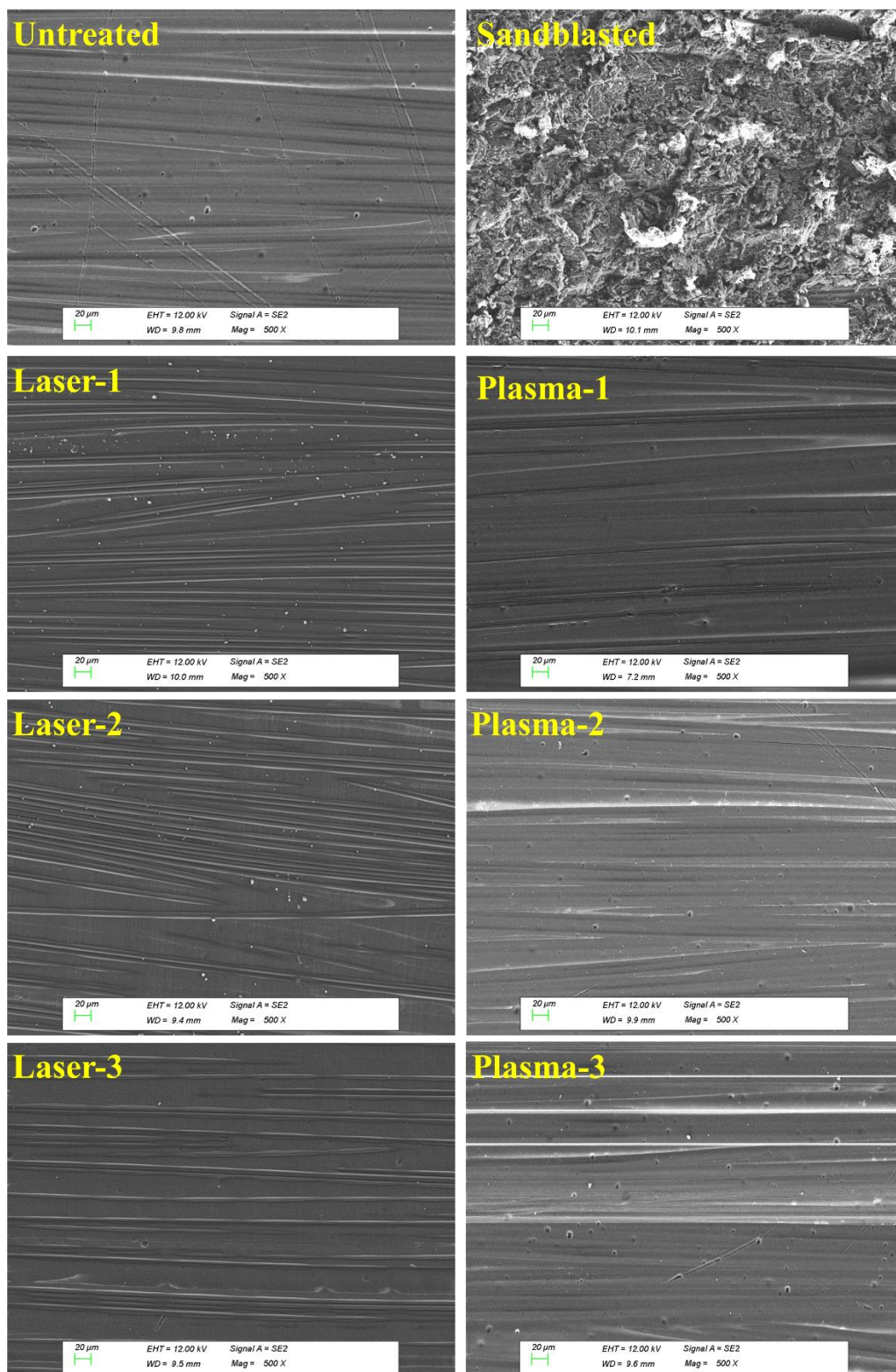
Figure 3.2 Examples of the SEM images for the Untreated and Treated PPS/CF surfaces (Magnification = 500X).

3.2.3 XPS Analyses of the Untreated and Treated Surfaces

Chemistry of the composite laminate surfaces is another important factor for the adhesion of primer paints. Thus, XPS analyses were conducted on the both resin rich and fiber rich regions of Untreated and Treated PPS/CF surfaces. Figure 3.3 indicated that XPS spectra of the Untreated sample, i.e. PPS matrix basically consisted of three elements; carbon (C 1s) at 285.1 eV, sulphur (S 2p) at 164.1 eV, and oxygen (O1s) at 532.1 eV, which are consistent with the previous studies [19, 35, 36]. Figure 3.3 revealed that for the Sandblasted and all Laser treated samples no new peaks appeared, but in the Plasma treated samples a minor peak for nitrogen (N 1s) at 402.1 eV formed. It can be found that the appearance of the oxygen peak on Untreated and Sandblasted surfaces can be attributed to the oxidation of PPS chains to promote crosslinking during the oxidation process.

In order to observe changes in the chemistry of the treated surfaces, elemental compositions (in atomic percentages) were tabulated in Table 3.3. It should be noted that these values are average of the "resin-rich" and "fiber-rich" regions evaluated. Moreover, to reveal oxidation status of the main elements of carbon and sulphur in PPS matrix, O/C and O/S atomic ratios were also determined.

It was seen that both O/C and O/S atomic ratios of the Untreated sample remained almost unchanged in the Laser treated samples; contrarily, significant increases were observed in the Plasma treated samples.

For example, O/C atomic ratio of the Untreated surface increased from 0.059 to 0.543 in the Plasma-1 treated surface, while this increase in O/S atomic ratio was from 0.372 up to 2.498. Thus, it could be interpreted that both C and S elements in the PPS structure oxidized significantly after Plasma treatments.

Table 3.3 Elemental compositions together with O/C and O/S atomic ratios of the Untreated and Treated PPS/CF surfaces determined by XPS analyses.

	C (at %)	O (at %)	S (at %)	N (at %)	O/C	O/S
Untreated	81	4.8	12.9	-	0.059	0.372
Sandblasted	77	11.6	7.5	-	0.151	1.540
Laser-1	82	5.8	11.5	-	0.070	0.503
Laser-2	82	4.2	13.6	-	0.051	0.305
Laser-3	83	3.2	14.3	-	0.039	0.225
Plasma-1	53	28.5	11.4	7.2	0.543	2.498
Plasma-2	64	21.2	10.0	4.4	0.331	2.109
Plasma-3	66	19.9	9.7	3.9	0.304	2.066
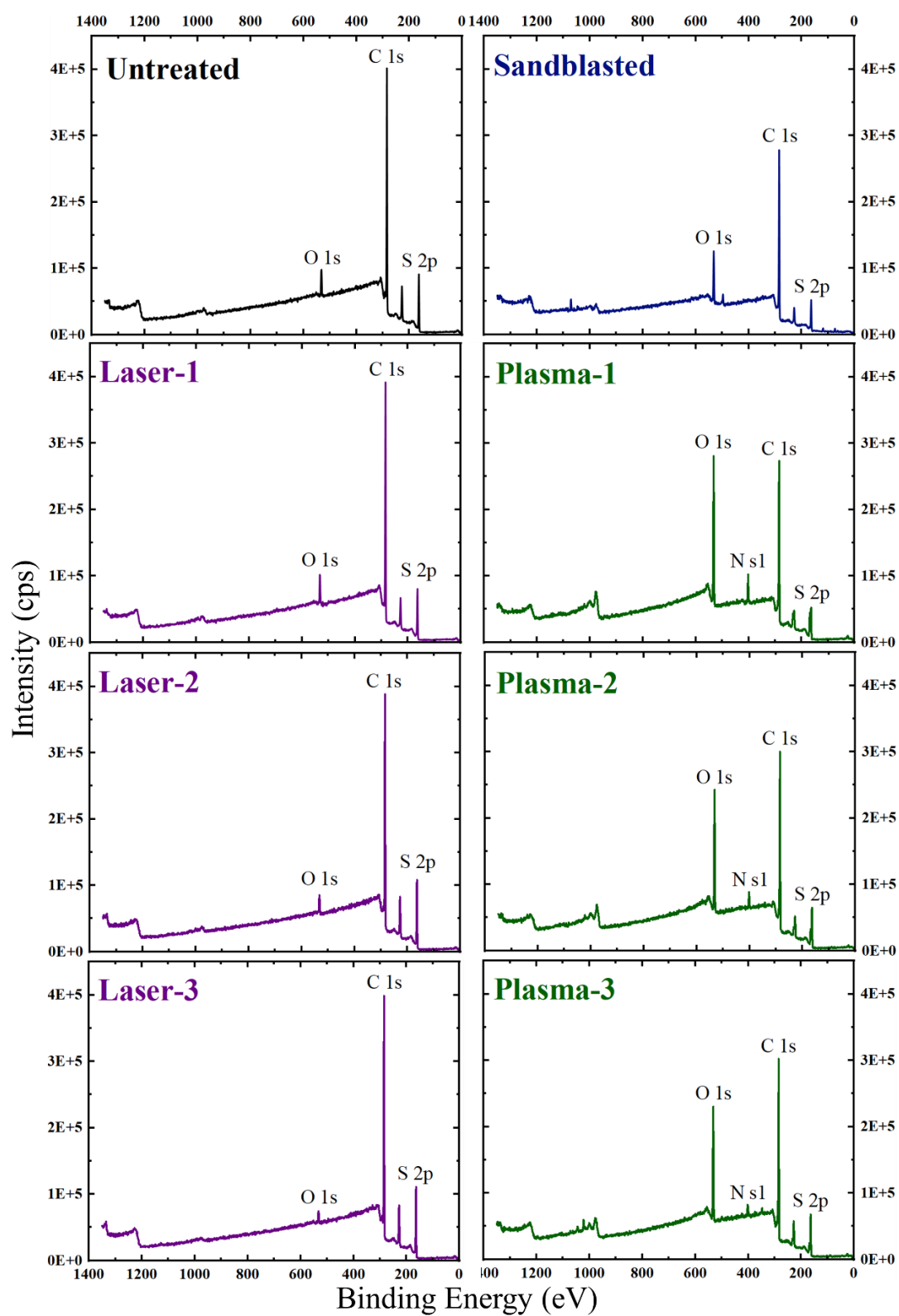
Figure 3.3 XPS spectra of the Untreated and Treated PPS/CF surfaces.
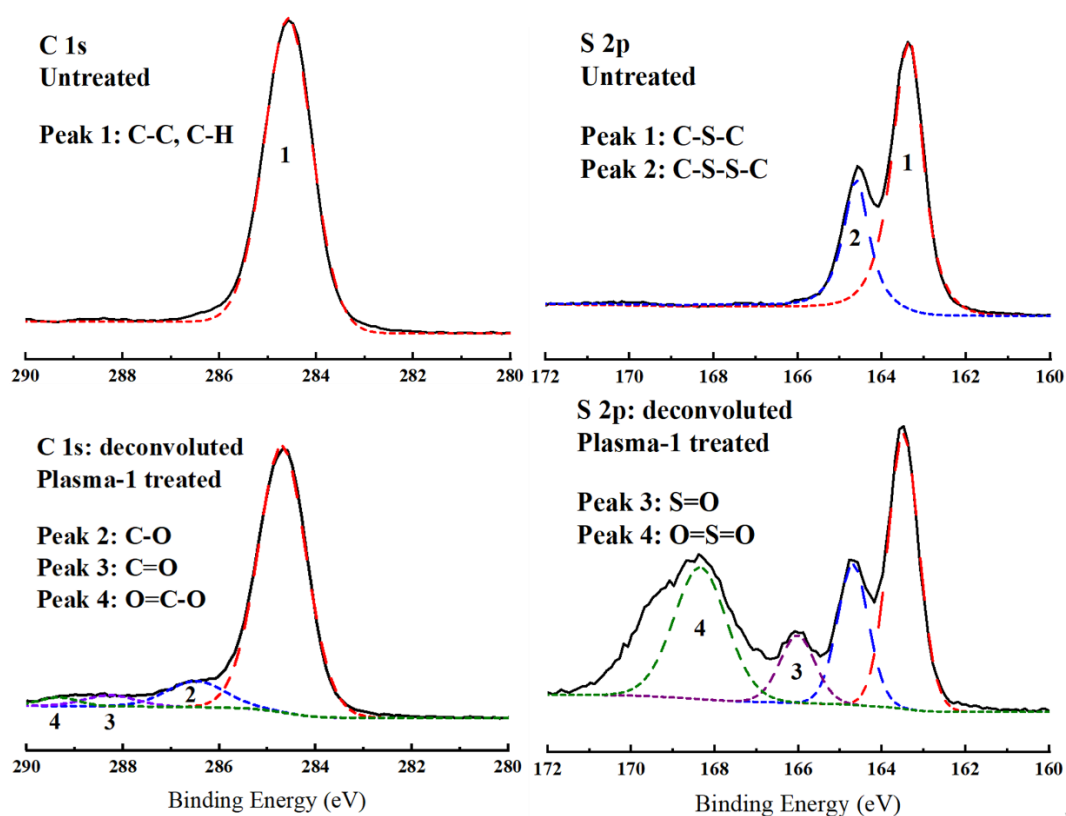
Figure 3.4 Above: C 1s and S 2p peaks of Untreated sample.
Below: Deconvoluted C 1s and S 2p peaks of Plasma-1 treated sample.

Consequently, to reveal these oxidized polar groups on the surfaces of Plasma treated samples, both C 1s and S 2p main peaks were deconvoluted. Figure 3.4 compares C 1s and S 2p main peaks of the Untreated sample and their deconvoluted form for the Plasma-1 treated sample. It was observed that Plasma treatment resulted in formation of three new peaks under C 1s envelope, representing oxidation bonds of C-O at 286.6 eV, C=O at 288.3 eV, and O=C-O at 289.4 eV. Similarly, in S 2p deconvolution, two new peaks were appeared under its envelope, representing the oxidation bonds of S=O at 166.1 eV and O=S=O at 168.4 eV.

Therefore, it could be pointed out that Plasma surface treatment increased the number of polar groups on the PPS/CF surfaces, which might improve primer paint adhesion.

3.2.4 FT-IR Analyses of the Untreated and Treated Surfaces

FT-IR analysis was the second technique used for the chemical characterization of the Untreated and Treated PPS/CF surfaces. As shown in Figure 3.5, it was observed that there were no apparent differences between the spectrum of Untreated sample and spectra of the Laser treated samples. Then, due to higher possibility of changes in the Plasma treated samples, spectrum of Untreated and Plasma-1 treated samples were compared in Figure 3.6 in detail by magnifying the scales of the axes.

The first spectrum in Figure 3.6 presents details of the typical peaks for the Untreated sample, i.e. PPS matrix. It is known that [3, 36, 37], characteristic IR peaks of PPS at 1573, 1470, 1384 cm^{-1} are attributed to the stretching vibration of C-C bonds in benzene ring, while the peak at 1091 cm^{-1} is assigned to the stretching vibration of the C-S bond. The strong peak at 807 cm^{-1} is the characteristic C-H of the benzene ring.

The second spectrum in Figure 3.6 was constructed by magnifying the scales of the Plasma-1 sample spectrum in order to reveal possible changes due to the oxidation of PPS matrix. Batista *et. al.* [3] pointed out that the peaks around 1800-1600 cm^{-1} were attributed to the carbonyl (C=O) stretching, while the peaks around 1300-1100 cm^{-1} were for the C-O bonds formed during oxidation. In this study, tiny peaks for C=O appeared at 1646 cm^{-1}, while for C-O appeared at 1260 cm^{-1}. Moreover, Xing *et. al.* [36] discussed that after oxidation, peaks for the stretching vibration of –SO$_2$– and –SO– form at 1178 and 1075 cm^{-1}, respectively. In this study, these tiny peaks appeared at 1179 and 1074 cm^{-1}, respectively.

Thus, it could be stated that formation of these chemically reactive sites, i.e. C=O, C-O, –SO$_2$–, –SO–, after Plasma surface treatments, might improve primer paint adhesion on the PPS/CF composite laminates.
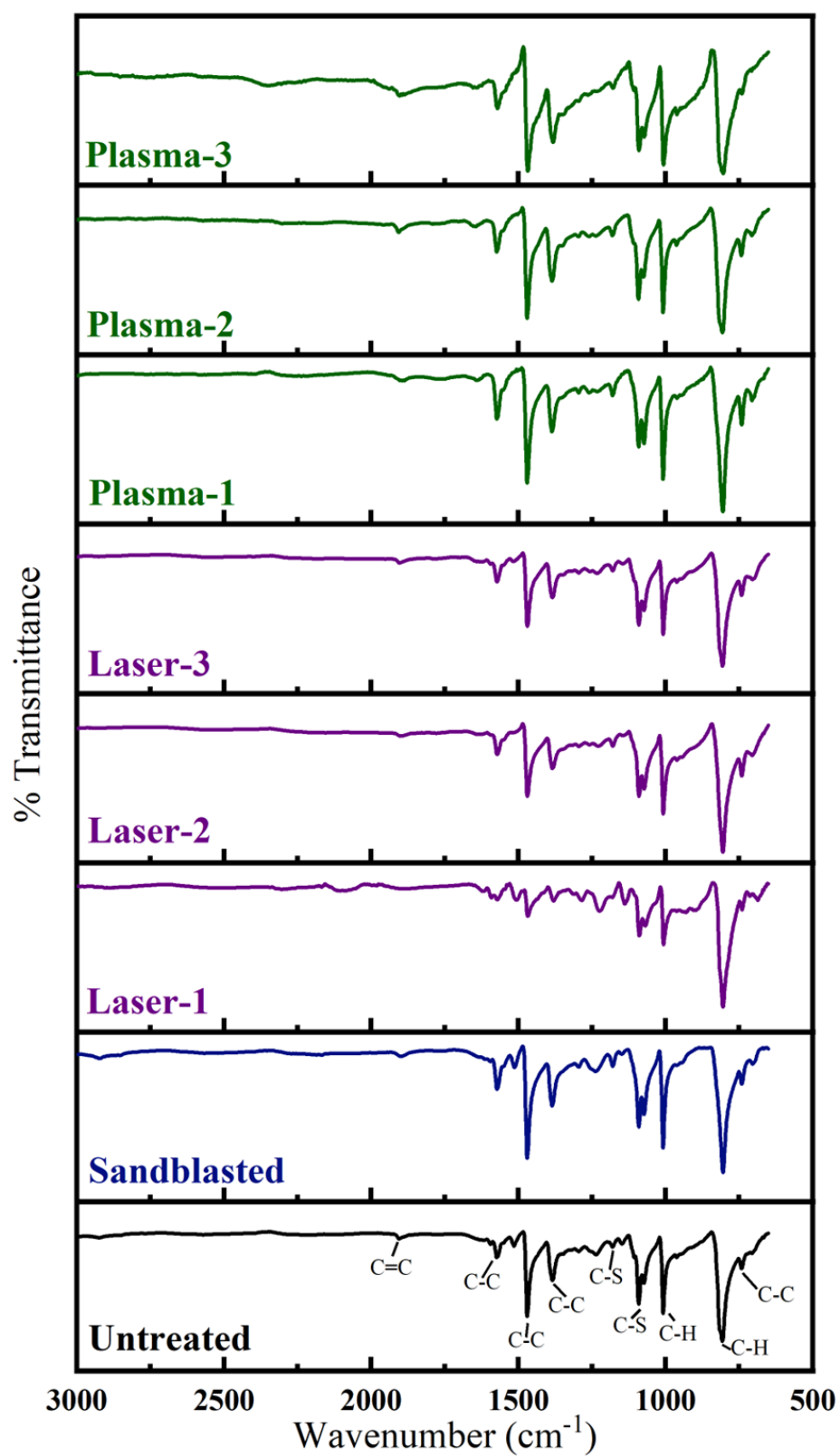
Figure 3.5 FT-IR spectra of the Untreated and Treated PPS/CF surfaces.
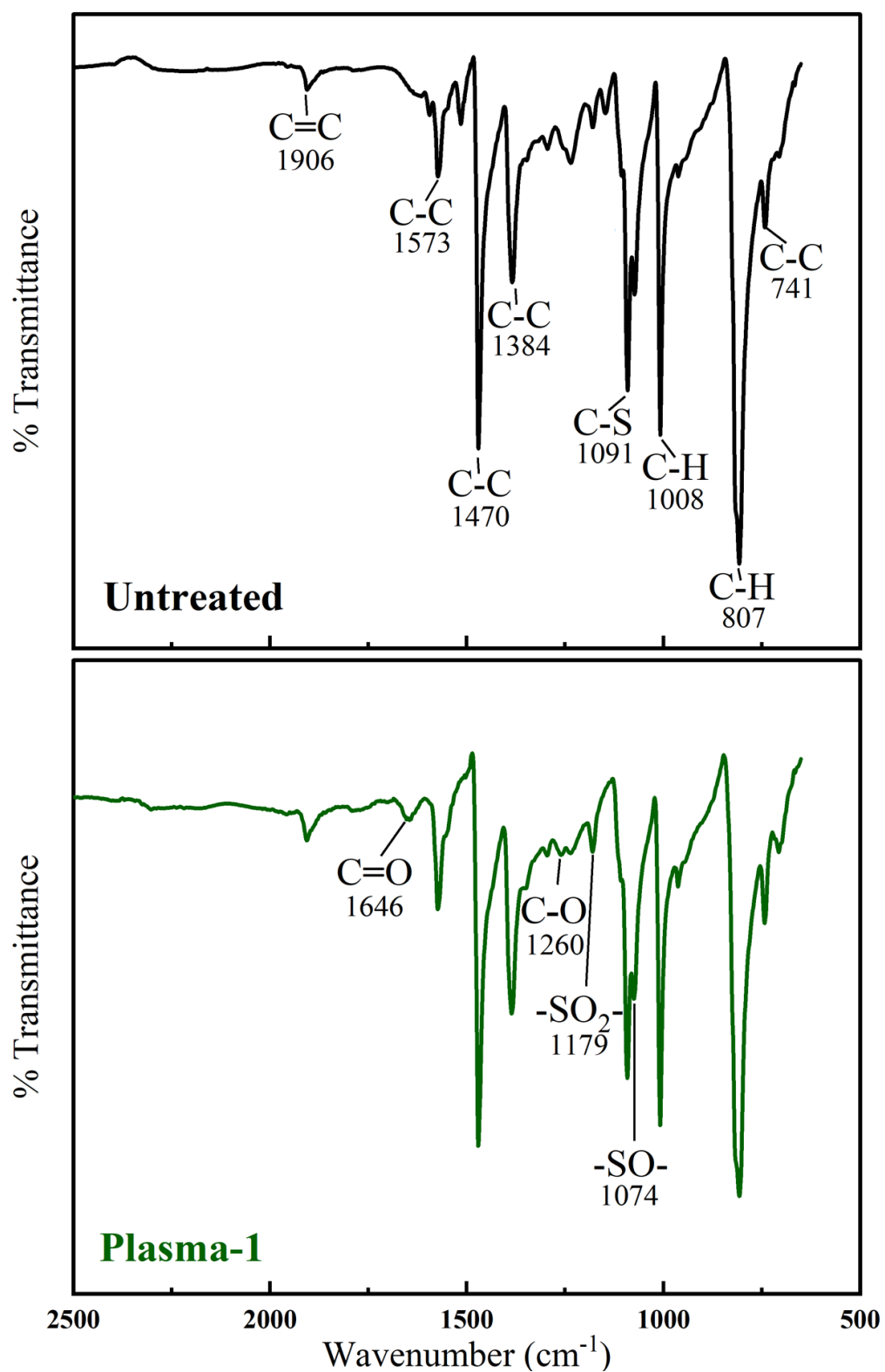
Figure 3.6 Details in the FT-IR spectrum of the Untreated and Plasma-1 treated PPS/CF surfaces.

3.3 Effects of Treatments on the Primer Paint Adhesion

After surface characterization of all untreated and treated PPS/CF composite laminates, primer paint adhesion on these surfaces were evaluated by conducting two different standardized industrial testing techniques, i.e. "cross-cut" and "three-point bending" adhesion tests. Results of these tests for all samples were illustrated in Figure 3.7 and Figure 3.8, separately. Then, their results were compared in Figure 3.9.

It should be pointed out that, in the industry, primer and top-coat paint adhesion tests were generally repeated for two conditions; the first one being just after the painting operations, while the second one is after immersing the painted specimens in water for a certain period. Because, testing after water immersion is considered to be very useful for predicting their service performance. Therefore in this study, all primer adhesion tests were first of all conducted for the samples just after primer painting operations, and these samples were designated as "before water immersion". Then, all tests were repeated for another group of primer painted samples which were this time immersed in deionized water for 7 days, thus those specimens were designated as "after water immersion".

3.3.1 Adhesion Performance According to Cross-cut Tests

As explained in Section 2.5 in detail, lattice patterns were cut into the primer paint layer by using a hand-held multi-blade cross-cutting device. Then, a kind of qualitative evaluation for the resistance of primer paint against separation from composite laminate surfaces were conducted. After cleaning the primer paint residues from the area of cutting, appearances of the lattice patterns were inspected under a magnifier, and then compared with adhesion grade classification table given by the standard (Table 2.1). Eventually, depending on the degree of primer paint flaking from the cross-cut lattice patterns, primer adhesion performance was graded as GT0, GT1, GT2, GT3, GT4, GT5. The "highest" or "best" adhesion grade is

assigned with GT0, while GT5 represents the "lowest" or "worst" adhesion grade; in which industrially acceptable adhesion grades are only GT0 and GT1.

Figure 3.7 illustrates appearances of the cross-cut lattice patterns for all untreated and treated sample surfaces "before" and "after" water immersion, together with their adhesion grades (GT) assigned by comparing the appearances given in the standard (Table 2.1). It was revealed that all surface treated (sandblasted, laser and plasma treated) PPS/CF samples, both "before" and "after" water immersion, were assigned with the "best" adhesion grade of GT0. On the other hand, due to the significant degree of primer paint separation, i.e. large amount of detachment of primer paint flakes from their cross-cut lattices, Untreated samples were assigned with very low adhesion grades, being only GT4 and GT2 for the "before" and "after" water immersed samples, respectively.

Before Water Immersion

Untreated — GT4	Sandblasted — GT0
Laser-1 — GT0	Plasma-1 — GT0
Laser-2 — GT0	Plasma-2 — GT0
Laser-3 — GT0	Plasma-3 — GT0

After Water Immersion

Untreated — GT2	Sandblasted — GT0
Laser-1 — GT0	Plasma-1 — GT0
Laser-2 — GT0	Plasma-2 — GT0
Laser-3 — GT0	Plasma-3 — GT0
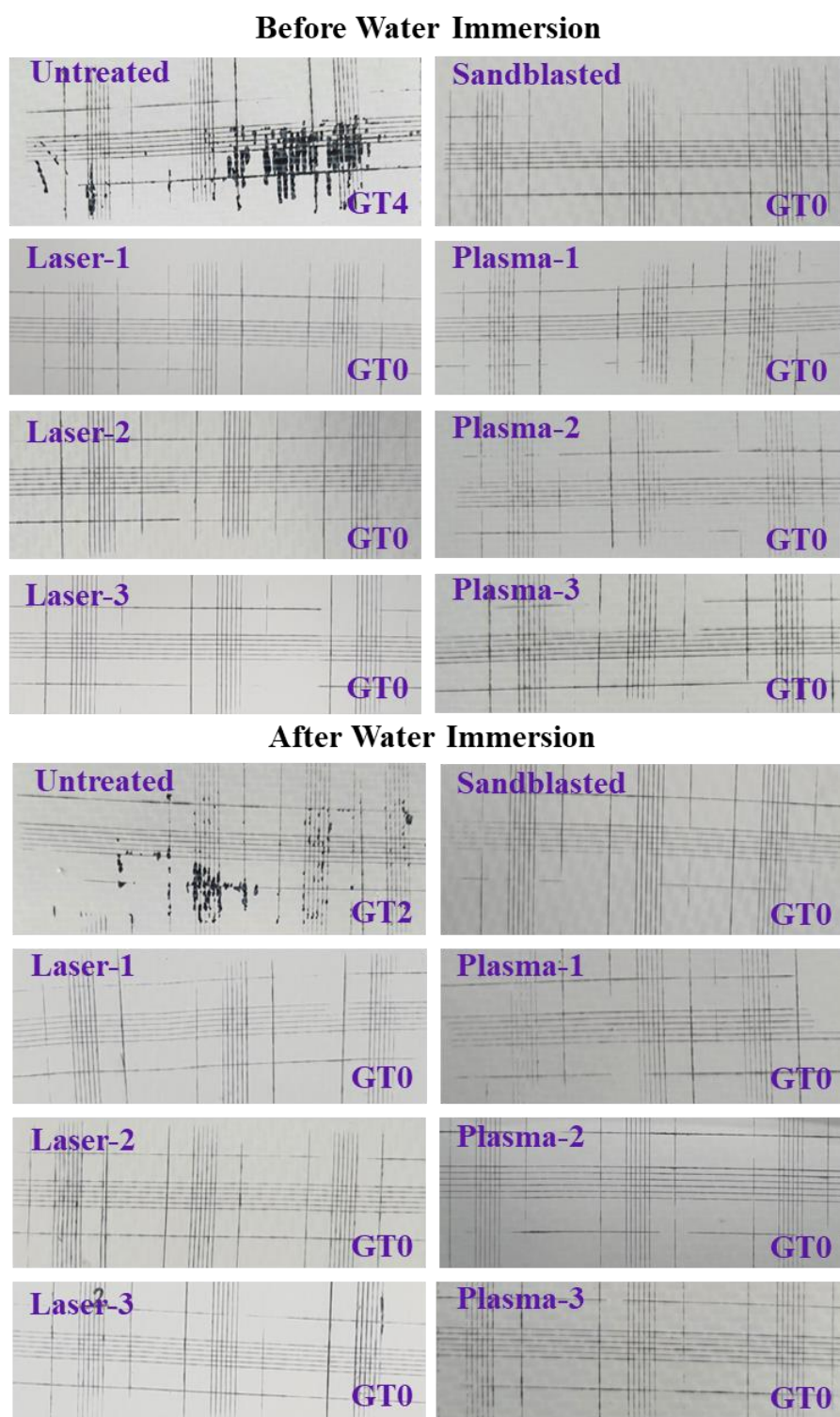
Figure 3.7 Appearances of the Cross-cut Lattice Patterns including assigned Adhesion Grades of Untreated and Treated PPS/CF surfaces "before" and "after" water immersion.

3.3.2 Adhesion Performance According to Three-point Bending Tests

In comparison to cross-cut adhesion test, three-point bending test is considered a more quantitative one for the determination of adhesion performance. As explained in Section 2.5 in detail, in order to evaluate resistance of the primer paint against separation from the composite laminate surfaces, a smaller thermosetting rigid block was molded onto the center of three-point bending specimens prepared from the untreated and treated, and then primer painted PPS/CF samples. Then, the whole specimen was loaded until the start of separation of the primer paint layer together with the rigid block at the center. Eventually, adhesion performance of the primer paint was first evaluated qualitatively by visual inspection of the separated surfaces, and then quantitively by recording the maximum load (in Newtons) reached in the load-deflection curve.

Figure 3.8 illustrates appearances of the separated surfaces for all untreated and treated sample surfaces "before" and "after" water immersion. It should be noted that smaller images "above" indicate "surface of the thermosetting block" after separation, while larger images "below" indicate "surface of the PPS/CF samples" after separation. It was observed that for the Untreated sample, separated surface appeared almost "black" due to the characteristic appearance of woven carbon fibers. This could be interpreted that in the Untreated sample, primer paint adhesion on this surface was extremely poor, there was almost no residues of the "white" colored primer paint, i.e. the separation mechanism was "adhesive".

On the other hand, Figure 3.8 revealed that, for all surface treated (sandblasted, laser and plasma treated) PPS/CF samples, both "before" and "after" water immersion, separated surfaces appeared all "whitish" due to the large amount of white colored primer paint layer left on the separated surface. This could be interpreted that for all surface treated (sandblast, laser, plasma) samples, primer paint adhesion performance was very good. Since both of the separated surfaces appeared whitish due to the applied primer paint layer remained on both surfaces, the separation mechanism could be defined as "cohesive".

In Figure 3.8, values of Maximum Load reached at the Start of Separation were also indicated. That parameter in this study is named as "Separation Load". These values with standard deviations were compared in Figure 3.9. It was observed that compared to the Separation Load reached for the Untreated sample, significant increases could be obtained after all surface treatments. For instance, "before" water immersion case, Separation Load of the untreated sample increased from 75 N up to 245 N in Sandblasted sample, up to 237 N in Laser Treated samples, and up to 193 N in Plasma treated samples; i.e. the increases being more than three times. For the "after" water immersion case, these increases were from 103 N up to 260 N, 269 N, and 224 N, respectively; i.e. the increases were more than two times.

Figure 3.8 and Figure 3.9 also revealed that the values of the Separation Load obtained for all untreated and treated samples "after" water immersion case were all higher compared to the "before" water immersion case. In the literature [31, 32] similar observations were made for the PEEK/CF and PAEK/CF thermoplastic composite laminate samples. Although the mechanisms involved for this behavior is still unclear, it could be generally speculated that water immersion could increase primer paint adhesion due to the certain changes in the chemical structure of primer paints.
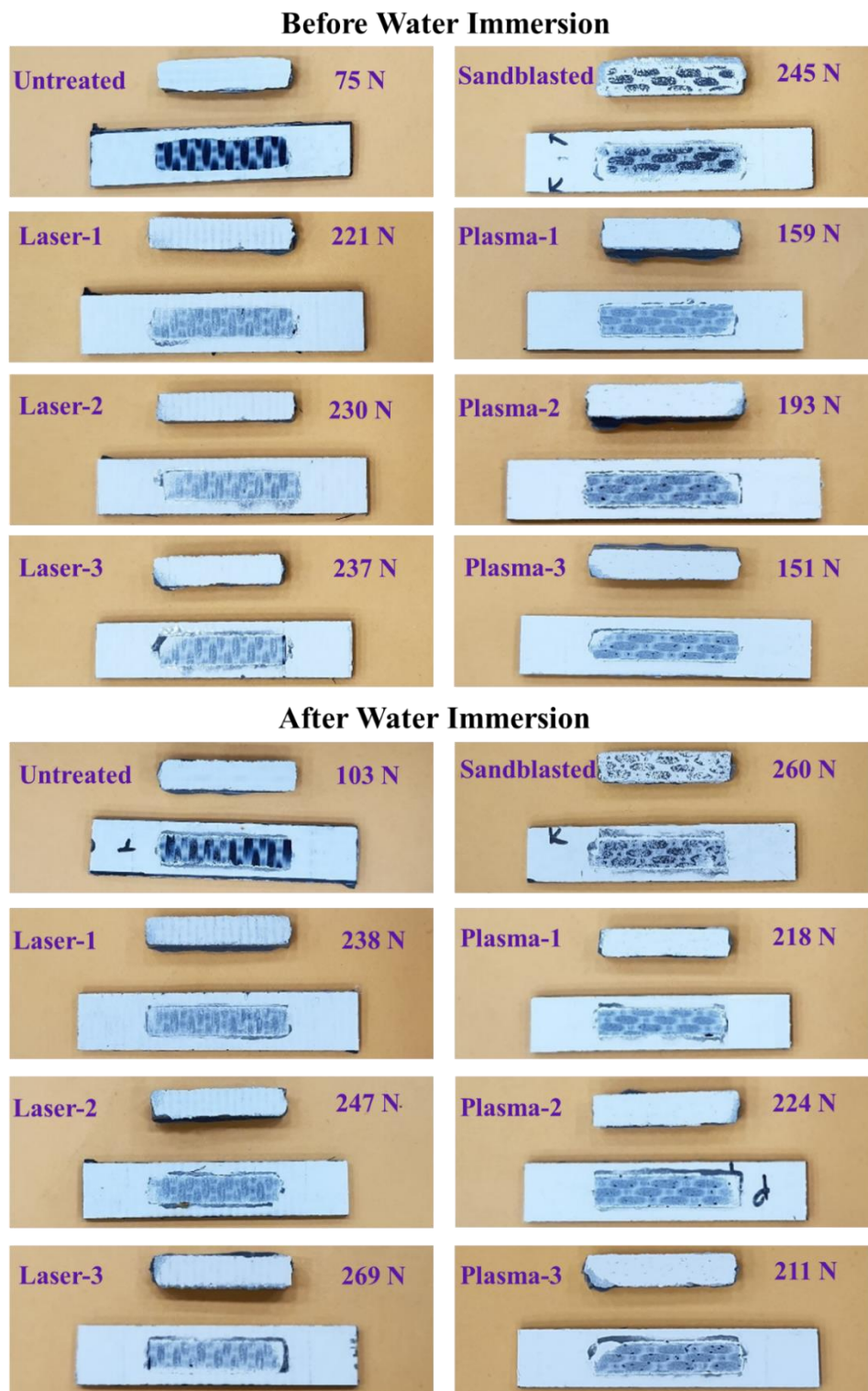
Figure 3.8 Appearances of the Separated Surfaces including maximum Separation Loads obtained by Three-point Bending tests of Untreated and Treated PPS/CF surfaces "before" and "after" water immersion.
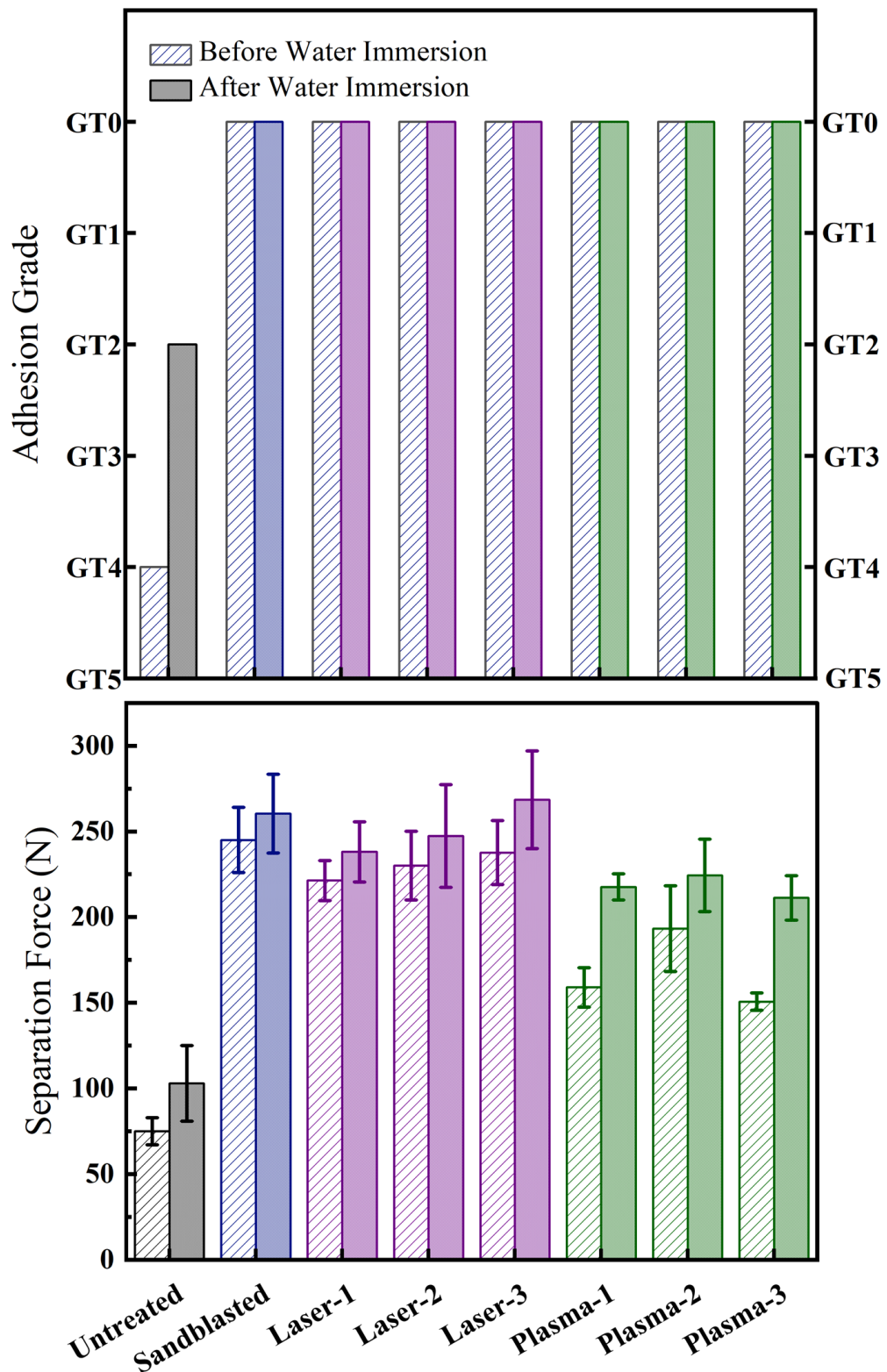
Figure 3.9 Comparison of Cross-cut and Three-point Bending adhesion tests results for Untreated and Treated PPS/CF surfaces "before" and "after" water immersion.

CHAPTER 4

CONCLUSIONS

Specific and general conclusions drawn from the surface characterization analyses and primer paint adhesion tests conducted for the untreated, sandblasted, laser treated and plasma treated PPS/CF thermoplastic composite laminate samples were as fallows.

(i)   Specific Conclusions

- Wettability analyses showed that all surface treatments decreased "Water Contact Angle" values, while increased "Total Surface Free Energy" values, significantly. However, the increase in "Polar Component" of total surface energy was significant only in the Plasma treated samples.

- SEM analyses indicated that enormous degree of "surface roughness" formed only in the Sandblasted sample with certain degree of "fiber stripping" and "fiber damage".

- XPS and FT-IR analyses revealed that formation of chemically reactive sites via oxidation of Carbon and Sulphur elements in the PPS structure occurred especially in the Plasma treated samples.

- According to Cross-cut Adhesion tests, all surface treated samples were assigned with the "best" primer adhesion grade of GT0.

- According to Three-point Bending Adhesion tests, all surface treated samples reached at least two times more maximum Separation Load with "cohesive" separation mechanism of primer paint layers.

(ii)   General Conclusions

The success of the Sandblasted samples could be attributed to the increased micro-level surface roughness, while for the Laser treated samples nano-level surface roughness, both of them leading to decreased Contact Angle values, and increased Total Surface Free Energy values.

The success of the Plasma treated samples could be attributed to the increased number of chemically reactive sites formed by the oxidation of Carbon and Sulphur elements in PPS matrix.

On the other hand, although traditional Sandblasting method resulted in high levels of Primer Paint Adhesion on the PPS/CF surfaces, it would be not advised. Because, this rather manual traditional technique cannot eliminate human mistakes leading to significant degree of inconsistencies. It could also harm bulk composite laminate and fibers on the surfaces leading to flaws and delamination. Moreover, sandblasting produce a lot of dust, which if trapped under the primer paint layer, results in poor adhesion.

Therefore, in order to prevent these problems, rather automated robotic techniques of Laser or Plasma surface treatments would be advisable for the paint-shops of PPS/CF composite laminates.

REFERENCES

[1] Liu, Y., Zhou, X., & Wang, Z. (2020). Effect of isothermal heat treatment on crystallinity, tensile strength and failure mode of CF/PPS Laminate. *High Performance Polymers*, *33*(5), 497–508. https://doi.org/10.1177/0954008320969843

[2] Polyphenylene sulfide (PPS) - A robust polymer with multiple applications: Polymers from Poly Fluoro Ltd. Poly Fluoro Ltd. (n.d.). Retrieved March 13, 2023, from https://polyfluoroltd.com/blog/polyphenylene-sulfide-pps-a-robust-polymer-with-multiple-applications

[3] Batista, N. L., Olivier, P., Bernhart, G., Rezende, M. C., & Botelho, E. C. (2016). Correlation between degree of crystallinity, morphology and mechanical properties of PPS/Carbon Fiber Laminates. *Materials Research*, *19*(1), 195–201. https://doi.org/10.1590/1980-5373-mr-2015-0453

[4] Perng, L. H. (2000). Thermal decomposition characteristics of poly(phenylene sulfide) by stepwise PY-GC/MS and TG/Ms Techniques. *Polymer Degradation and Stability*, *69*(3), 323–332. https://doi.org/10.1016/s0141-3910(00)00077-x

[5] Mallick, P. K. (2010). Thermoplastics and thermoplastic–matrix composites for lightweight automotive structures. In *Materials, design and manufacturing for Lightweight Vehicles*. essay, CRC Press.

[6] Seo, K. H., Park, L. S., Baek, J. B., & Brostow, W. (1993). Thermal behaviour of poly (phenylene sulfide) and its derivatives. *Polymer*, *34*(12), 2524–2527. https://doi.org/10.1016/0032-3861(93)90583-v

[7]   Chen, G., Mohanty, A. K., & Misra, M. (2021). Progress in research and applications of polyphenylene sulfide blends and composites with carbons. *Composites Part B: Engineering*, *209*, 108553. https://doi.org/10.1016/j.compositesb.2020.108553

[8]   Hughes, R. G. B. A. E., Mol, J. M. C., & Zheludkevich, M. L. (2016). Active protective coatings: New-generation coatings for metals (Vol. 233, pp. 59-84). Springer, Dordrecht, Netherlands. https://doi.org/10.1007/978-94-017-7540-3_4.

[9]   Li, S., Sun, T., Liu, C., Yang, W., & Tang, Q. (2018). A study of laser surface treatment in bonded repair of composite aircraft structures. *Royal Society Open Science*, *5*(3), 171272. https://doi.org/10.1098/rsos.171272

[10]   Schmutzler, H., Popp, J., Büchter, E., Wittich, H., Schulte, K., & Fiedler, B. (2014). Improvement of bonding strength of scarf-bonded carbon fibre/epoxy laminates by Nd:YAG Laser Surface Activation. *Composites Part A: Applied Science and Manufacturing*, *67*, 123–130. https://doi.org/10.1016/j.compositesa.2014.08.029

[11]   Fischer, F., Kreling, S., Jäschke, P., Frauenhofer, M., Kracht, D., & Dilger, K. (2012). Laser surface pre-treatment of CFRP for adhesive bonding in consideration of the absorption behaviour. *The Journal of Adhesion*, *88*(4-6), 350–363. https://doi.org/10.1080/00218464.2012.660042

[12]   Obilor, A. F., Pacella, M., Wilson, A., & Silberschmidt, V. V. (2022). Micro-texturing of polymer surfaces using lasers: A Review. *The International Journal of Advanced Manufacturing Technology*, *120*(1-2), 103–135. https://doi.org/10.1007/s00170-022-08731-1

[13]   Mittal, K. L., Bahners, T., Buchman, A., Rotel, M., & Dodiuk-Kenig, H. (2015). Nd:YAG Laser Surface Treatment of Various Materials to Enhance Adhesion. In *Laser surface modification and adhesion* (pp. 3–54). essay, New York, NY: John Wiley & Sons.

[14]   Dupuis, A., Ho, T. H., Fahs, A., Lafabrier, A., Louarn, G., Bacharouche, J., Airoudj, A., Aragon, E., & Chailan, J.-F. (2015). Improving adhesion of powder coating on peek composite: Influence of atmospheric plasma parameters. *Applied Surface Science*, *357*, 1196–1204. https://doi.org/10.1016/j.apsusc.2015.09.148

[15]   Noeske, M., Degenhardt, J., Strudthoff, S., & Lommatzsch, U. (2004). Plasma jet treatment of five polymers at atmospheric pressure: Surface modifications and the relevance for adhesion. *International Journal of Adhesion and Adhesives*, *24*(2), 171–177. https://doi.org/10.1016/j.ijadhadh.2003.09.006

[16]   Zaldivar, R. J., Kim, H. I., Steckel, G. L., Nokes, J. P., & Morgan, B. A. (2009). Effect of processing parameter changes on the adhesion of plasma-treated carbon fiber reinforced epoxy composites. *Journal of Composite Materials*, *44*(12), 1435–1453. https://doi.org/10.1177/0021998309355846

[17]   Lee, H., Ohsawa, I., & Takahashi, J. (2015). Effect of plasma surface treatment of recycled carbon fiber on carbon fiber-reinforced plastics (CFRP) interfacial properties. *Applied Surface Science*, *328*, 241–246. https://doi.org/10.1016/j.apsusc.2014.12.012

[18]   Lu, Qiu, Lu, Wang, Xiao, Zheng, Wang, & Zhang. (2019). Enhancing the interfacial strength of carbon fiber/poly(ether ether ketone) hybrid composites by plasma treatments. *Polymers*, *11*(5), 753. https://doi.org/10.3390/polym11050753

[19] Xu, D., Liu, B., Zhang, G., Long, S., Wang, X., & Yang, J. (2015). Effect of air plasma treatment on interfacial shear strength of carbon fiber–reinforced polyphenylene sulfide. *High Performance Polymers*, *28*(4), 411–424. https://doi.org/10.1177/0954008315585012

[20] Han, P., Butterfield, J., Price, M., Buchanan, S., & Murphy, A. (2013). Experimental investigation of thermoforming carbon fibre-reinforced polyphenylene sulphide composites. *Journal of Thermoplastic Composite Materials*, *28*(4), 529–547. https://doi.org/10.1177/0892705713486133

[21] Abbassi, F., Elfaleh, I., Mistou, S., Zghal, A., Fazzini, M., & Djilali, T. (2011). Experimental and numerical investigations of a thermoplastic composite (carbon/PPS) thermoforming. *Structural Control and Health Monitoring*, *18*(7), 769–780. https://doi.org/10.1002/stc.491

[22] Grouve, W. J. B., Warnet, L. L., Rietman, B., Visser, H. A., & Akkerman, R. (2013). Optimization of the tape placement process parameters for carbon–PPS Composites. *Composites Part A: Applied Science and Manufacturing*, *50*, 44–53. https://doi.org/10.1016/j.compositesa.2013.03.003

[23] Grouve, W. J. B., Warnet, L. L., Rietman, B., & Akkerman, R. (2012). On the weld strength of in situ tape placed reinforcements on weave reinforced structures. *Composites Part A: Applied Science and Manufacturing*, *43*(9), 1530–1536. https://doi.org/10.1016/j.compositesa.2012.04.010

[24] Reynolds, N., Awang-Ngah, S., Williams, G., & Hughes, D. J. (2020). Direct processing of structural thermoplastic composites using rapid isothermal stamp forming. *Applied Composite Materials*, *27*(1-2), 107–115. https://doi.org/10.1007/s10443-020-09797-4

[25] Ma, C.-C. M., Yn, M.-S., Chen, C.-H., & Chiang, C.-L. (1990). Processing and properties of Pultruded Thermoplastic Composites (I). *Composites Manufacturing*, *1*(3), 191–196. https://doi.org/10.1016/0956-7143(90)90167-u

[26] Rotel, M., Zahavi, J., Buchman, A., & Dodiuk, H. (1995). Preadhesion laser surface treatment of carbon fiber reinforced peek composite. *The Journal of Adhesion*, *55*(1-2), 77–97. https://doi.org/10.1080/00218469509342408

[27] Ledesma, R. I., Palmieri, F. L., Lin, Y., Belcher, M. A., Ferriell, D. R., Thomas, S. K., & Connell, J. W. (2020). Picosecond laser surface treatment and analysis of thermoplastic composites for structural adhesive bonding. *Composites Part B: Engineering*, *191*, 107939. https://doi.org/10.1016/j.compositesb.2020.107939

[28] Genna, S., Leone, C., Ucciardello, N., & Giuliani, M. (2017). Increasing adhesive bonding of carbon fiber reinforced thermoplastic matrix by laser surface treatment. *Polymer Engineering & Science*, *57*(7), 685–692. https://doi.org/10.1002/pen.24577

[29] Scarselli, G., Quan, D., Murphy, N., Deegan, B., Dowling, D., & Ivankovic, A. (2021). Adhesion improvement of thermoplastics-based composites by atmospheric plasma and UV treatments. *Applied Composite Materials*, *28*(1), 71–89. https://doi.org/10.1007/s10443-020-09854-y

[30] Iqbal, H. M. S., Bhowmik, S., & Benedictus, R. (2010). Surface modification of high performance polymers by atmospheric pressure plasma and failure mechanism of adhesive bonded joints. *International Journal of Adhesion and Adhesives*, *30*(6), 418–424. https://doi.org/10.1016/j.ijadhadh.2010.02.007

[31]   Brès, L., Sanchot, A., Rives, B., Gherardi, N., Naudé, N., & Aufray, M. (2019). Fine-tuning of chemical and physical polymer surface modifications by atmospheric pressure post-discharge plasma and its correlation with adhesion improvement. *Surface and Coatings Technology*, *362*, 388–396. https://doi.org/10.1016/j.surfcoat.2019.01.102

[32]   Lapena, M. H., & Lopes, C. M. (2022). Improvement of aerospace thermoplastic composite adhesion to coating with dielectric barrier discharge atmospheric pressure plasma surface treatment. *Plasma Processes and Polymers*, *20*(1), 2200081. https://doi.org/10.1002/ppap.202200081

[33]   Comyn, J. (1992). Contact angles and adhesive bonding. *International Journal of Adhesion and Adhesives*, *12*(3), 145–149. https://doi.org/10.1016/0143-7496(92)90045-w

[34]   Al-Maliki, H., Zsidai, L., Samyn, P., Szakál, Z., Keresztes, R., & Kalácska, G. (2017). Effects of atmospheric plasma treatment on adhesion and tribology of aromatic thermoplastic polymers. *Polymer Engineering & Science*, *58*(S1), 93-103. https://doi.org/10.1002/pen.24689

[35]   Cvelbar, U., Mozetič, M., Junkar, I., Vesel, A., Kovač, J., Drenik, A., Vrlinič, T., Hauptman, N., Klanjšek-Gunde, M., Markoli, B., Krstulović, N., Milošević, S., Gaboriau, F., & Belmonte, T. (2007). Oxygen plasma functionalization of poly(P-Phenilene Sulphide). *Applied Surface Science*, *253*(21), 8669–8673. https://doi.org/10.1016/j.apsusc.2007.04.074

[36]   Xing, J., Xu, Z., & Deng, B. (2018). Enhanced oxidation resistance of polyphenylene sulfide composites based on montmorillonite modified by Benzimidazolium Salt. *Polymers*, *10*(1), 83. https://doi.org/10.3390/polym10010083

[37]   Zimmerman, D. A., Koenig, J. L., & Ishida, H. (1995). Infrared spectroscopic analysis of poly(p-phenylene sulfide). *Spectrochimica Acta Part A: Molecular and Biomolecular Spectroscopy*, *51*(13), 2397–2409. https://doi.org/10.1016/0584-8539(95)01408-x

APPENDICES

After producing PPS/CF thermoplastic composite laminates, their various properties were determined by conducting certain tests and analyses. First, in accordance with the related standards, specimens were cut from the laminate plates by using a diamond tip industrial cutter (*Diamond-3, 3515RS*) having a cooling unit; then, solvent cleaning was applied to remove cutting residues.

Characterization techniques used could be listed in three main groups: (i) microstructural, (ii) thermal and (iii) mechanical, as explained in Appendices A, B, C below. Note that, for the microstructural and thermal analyses at least 3 measurements were conducted; while for the mechanical tests at least 5 specimens were tested. All properties of the PPS/CF specimens determined from these characterization techniques were tabulated in Appendices A, B and C as the average values with ± standard deviations.

APPENDIX A

MICROSTRUCTURAL ANALYSES OF PPS/CF SPECIMENS

In this group, Ultrasonic NDI, Optical Microscopy, Fiber Volume Content, Water Uptake analyses were conducted as shown in Figure A.1.

Ultrasonic Non-Destructive Inspection:

First of all, PPS/CF laminates were inspected for the possibilities of void formation and delamination by evaluating the C-scan images obtained via an Automated Ultrasonic Through Transmission system (*ACCUBOT-Fill*) (Figure A.1 (a)).

Microscopic Analysis:

For microstructural observations and precise thickness measurements PPS/CF samples cut into 2 x 3 mm were first acrylic molded, surface grinded, polished; and then examinate under an inverted optical microscope (*Olympus GX53*) (Figure A.1 (b)).

Fiber Volume Content Analysis:

In order to determine fiber and matrix content of the PPS/CF samples, sulfuric acid and hydrogen peroxide "Solution Digestion" method as described in the Procedure- B of the ASTM D3171 standard was used (Figure A.1 (c)).

Water Uptake Analysis:

The degree of moisture absorption of the PPS/CF samples cut into 50 x 50 mm were evaluated in a climate chamber (*Weisstechnik*) set to 70°C and 85% RH in accordance to EN3615 standard (Figure A.1 (d)). Similarly, water absorption level

of the samples were evaluated in a water bath (*Isolab*) set to 70°C in accordance to EN2378 standard.

Results of these microstructural analyses were given in Figure A.2 while the properties determined were tabulated in Table A.1.
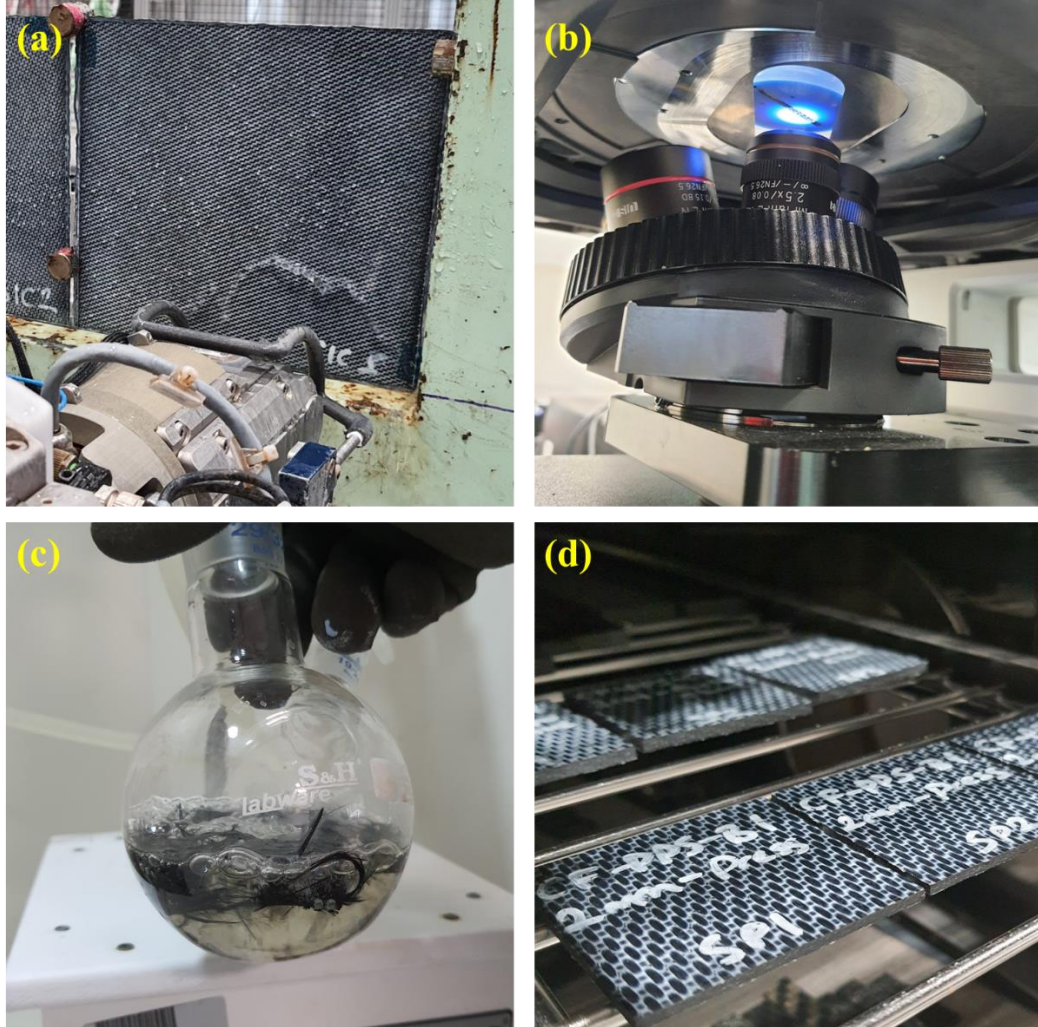
Figure A.1 Microstructural Analyses of PPS/CF Specimens: (a) Ultrasonic, (b) Microscopic, (c) Fiber Volume Content, and (d) Water Uptake Analyses.
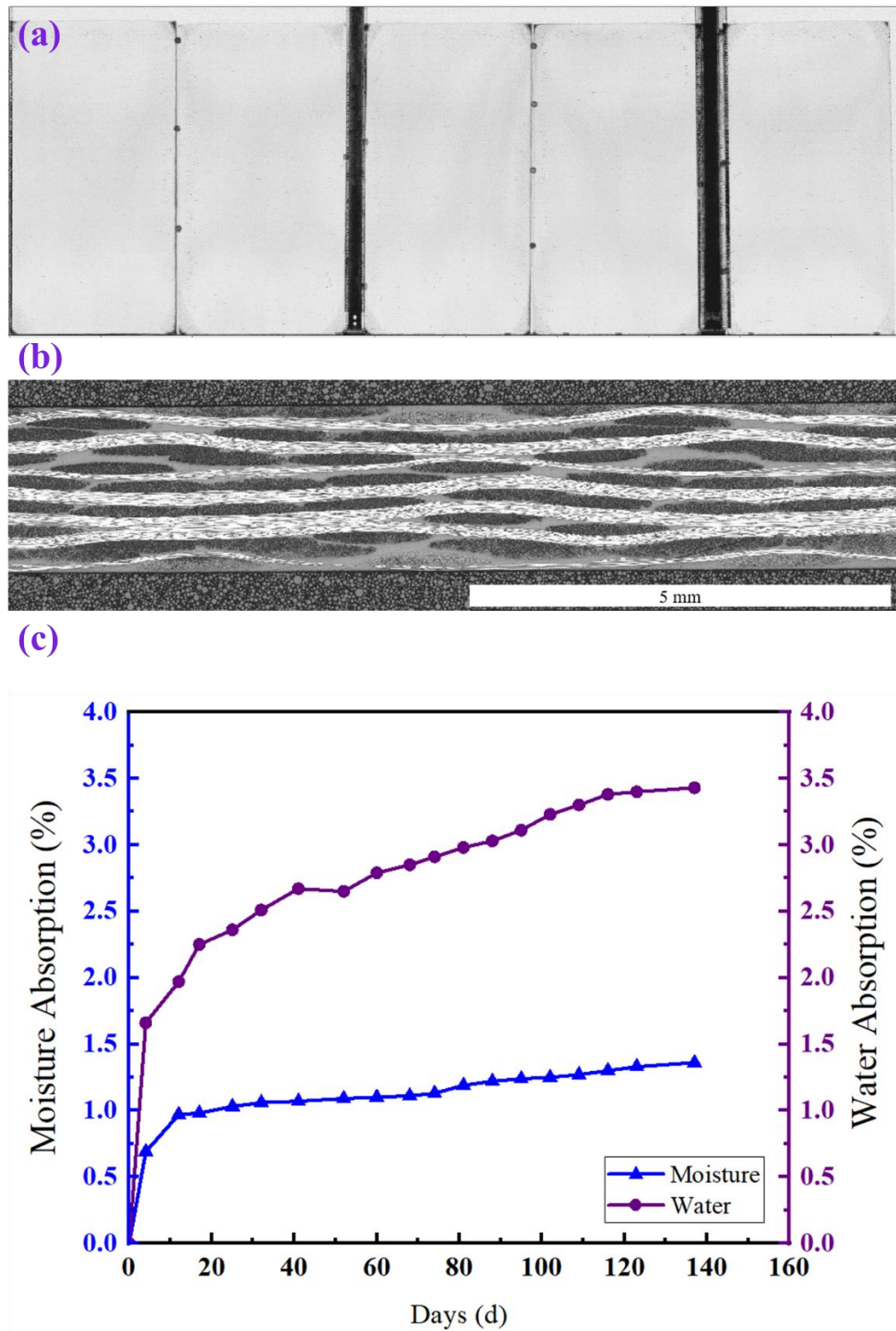
Figure A.2 Examples of the Microstructural Analyses conducted for PPS/CF laminate samples: (a) C-scan image from Ultrasonic Inspection, (b) Through thickness image from Optical Microscopy, and (c) Moisture and Water Uptake curves.

Table A.1 Properties of PPS/CF laminate samples determined from Microstructural Inspection and Analysis.

Analyses	Properties	Unit	Values
Ultrasonic Inspection	Macro Porosity	%	No apparent porosity
Optical Microscopy	Thickness	mm	1.96 ± 0.01
	Porosity	%	0.00
Acid Digestion	Fiber Content	vol%	51.97 ± 0.99
	Matrix Content	wt%	41.69 ± 1.49
	Density	kg/m^3	1.56 ± 0.01
Moisture Uptake	After 150 days	wt%	1.25 ± 0.11
Water Uptake	After 150 days	wt%	3.39 ± 0.61

APPENDIX B

THERMAL ANALYSES OF PPS/CF SPECIMENS

In this group, various thermal properties including glass transition temperature, matrix crystallinity, heat capacity, thermal degradation temperatures, thermal expansion coefficient, storage modulus, tan delta, conductivity, etc. were determined by conducting DSC, TGA, TMA, DMA and Thermal Diffusivity as shown in Figure B.1.

Differential Scanning Calorimetry (DSC):

DSC analyses (*TA Instruments, Q100*) was first of all used in order to determine especially glass transition temperature (T_g), and the degree of crystallinity (X_c) of the PPS matrix in the laminate under first heating profile from RT to 330°C at a rate of 10°C/min under nitrogen flow according to ASTM D3418 standard (Figure B.1 (a)). Sample mass was arranged as around 10 mg PPS matrix. The instrument was also used under sinusoidal modulated temperature mode of ±1°C amplitude at each 60 seconds, from RT to 250°C with 2°C/min ramp, in order to determine Heat Capacity (C_p) of the PPS matrix in accordance with ASTM E2716 standard. During matrix crystallinity calculations, ΔH_m^0 which is the melting enthalpy of 100% crystalline PPS matrix was taken as 150.4 J/g.

Thermogravimetric Analysis (TGA):

TG analyses (*Perkin Elmer, TGA 8000*) was especially conducted to determine thermal degradation temperature (T_d) of the PPS matrix of the laminate during the heating profile from RT to 850°C at a rate of 10°C/min under nitrogen flow, in accordance to ASTM E1131 standard (Figure B.1 (b)). Sample mass was arranged to have around 5 mg PPS matrix.

Thermomechanical Analysis (TMA):

Thermomechanical analysis (*TA Instruments, TMA 450*) was used to determine Thermal Expansion Coefficient of the PPS/CF samples cut into 5 x 5 x 5 mm, by measuring the dimensional changes along 3 axes during the heating profile from RT to 250°C at a rate of 5°C/min under nitrogen flow in accordance to ASTM E831 standard (Figure B.1 (c)).

Dynamic Mechanical Analysis (DMA):

Dynamic mechanical analysis (*TA Instruments, DMA Q800*) was conducted to observe Storage Modulus and Tan Delta (tan δ) values of the PPS/CF samples cut into 2 x 10 x 35 mm, under single cantilever loading from RT to 200°C at a heating rate of 5°C/min according to ASTM D4065 standard (Figure B.1 (d)).

Thermal Diffusivity Analysis:

Thermal diffusivity analyses (*Netzsch, LFA 647*) were carried out to determine Thermal Diffusivity of the PPS/CF samples cut into 10 x 10 mm according to ASTM E1461 standard. Specimen surfaces were first spray coated with a thin layer of graphite to eliminate energy reflection (Figure B.1 (e)). Radiant energy pulses (i.e. laser flash shots) were exposed starting from 25°C to 250°C with 25°C intervals (Figure B.1 (f)).

Note that, thermal conductivity of the PPS/CF samples were determined by using the values of Thermal Diffusivity (obtained from the above analyses), Specific Heat Capacity (obtained from the modulated DSC analyses), and the Density (obtained from Fiber Volume Content Analyses).

Examples of the curves obtained from these Thermal Analyses are given in Figure B.2, while the thermal properties determined are tabulated in Table B.1.
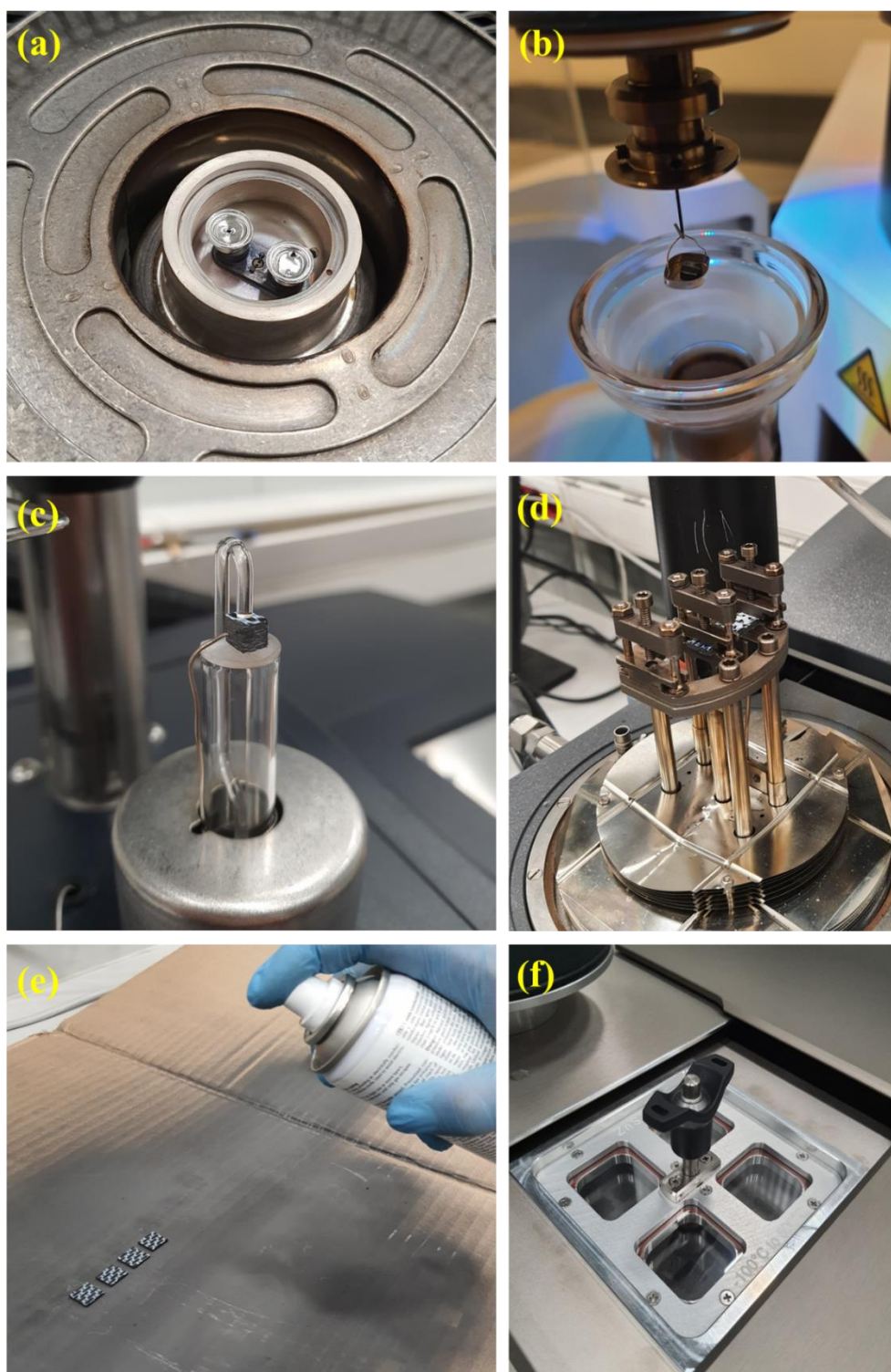
Figure B.1 Thermal Analyses of PPS/CF specimens: (a) DSC, (b) TGA, (c)TMA, (d) DMA, (e) and (f) Thermal Diffusivity Analyses.
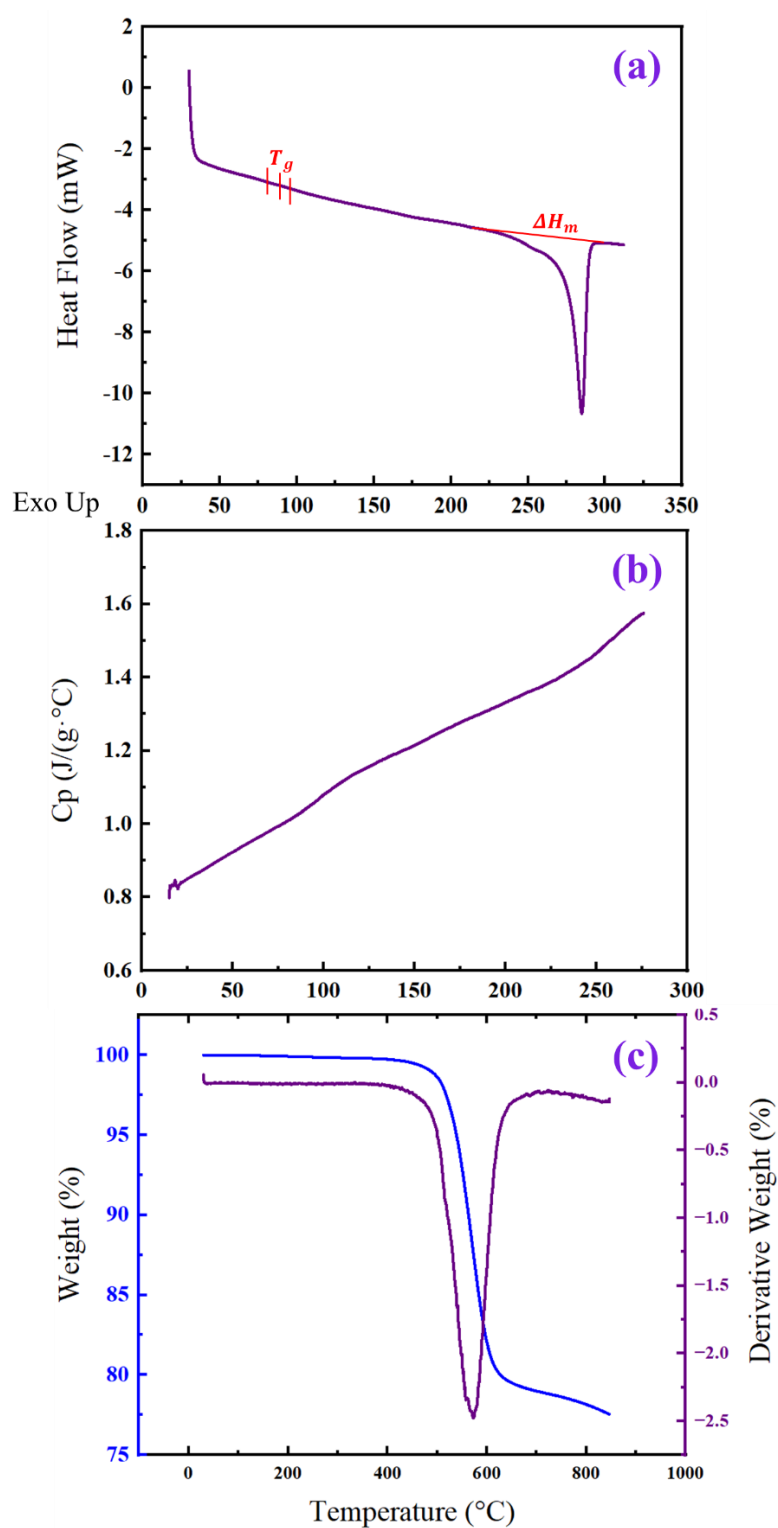
Figure B.2 Examples of the curves obtained during thermal analyses of PPS/CF samples: (a) DSC, (b) Modulated DSC, (c) TGA, (d) TMA, (e) DMA, and (f) Thermal Diffusivity and Conductivity.

74
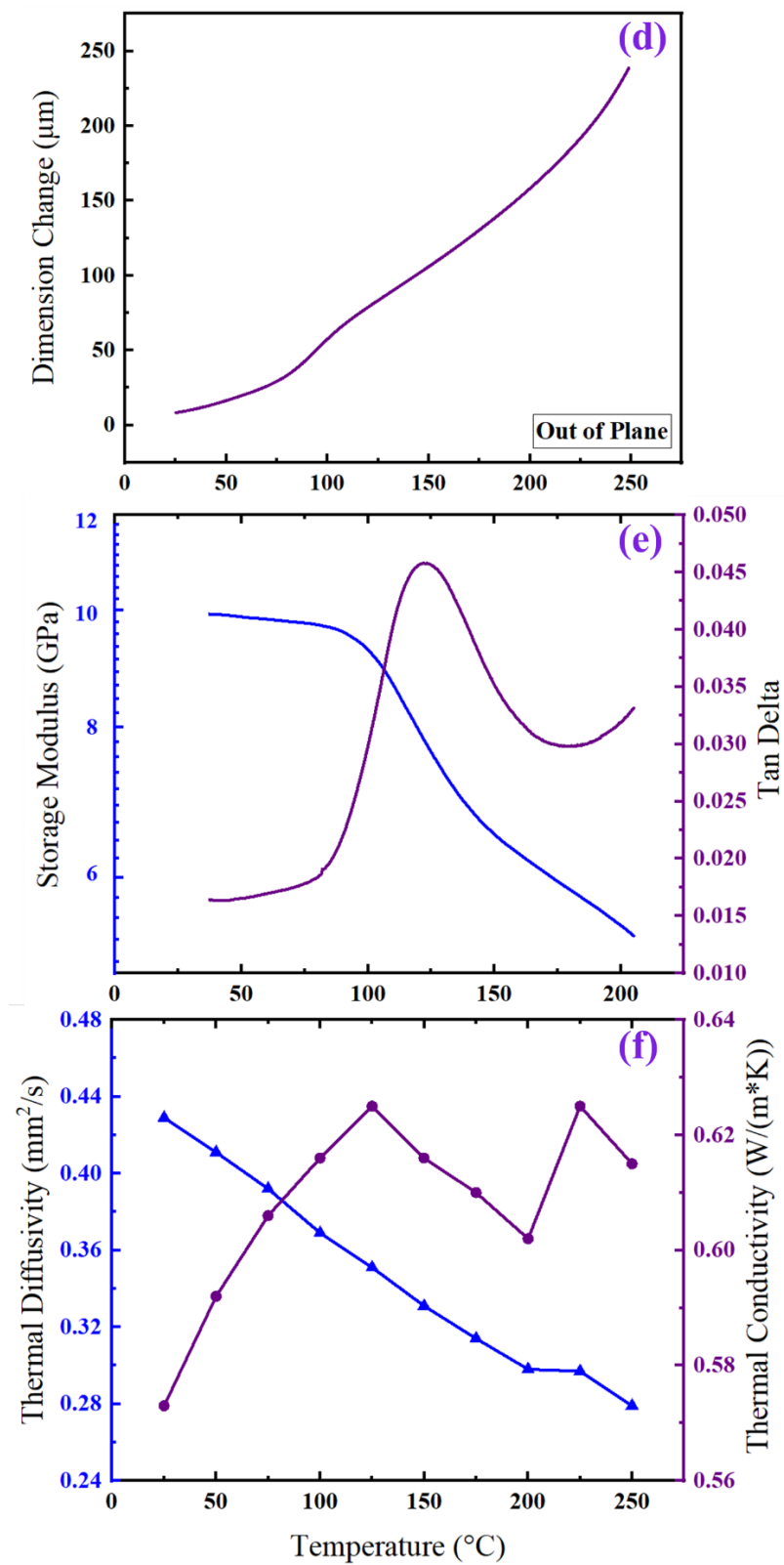
Figure B.2 (Continued.)

Table B.1 Thermal properties of PPS/CF samples determined from thermal analyses.

Analyses	Properties	Unit	Values
DSC	Glass Transition Temperature	°C	92.95 ± 2.21
	Crystallinity	%	23.24 ± 0.33
	Heat Capacity	J/g.°C	0.893 ± 0.30
TGA	Thermal Degradation Onset	°C	524 ± 4.34
	Max. Thermal Degradation	°C	575 ± 3.82
	Residue at 850°C	%	72 ± 5.23
TMA*	Thermal Expansion Coefficient In Plane 0°	µm/m.°C	12.66
	Thermal Expansion Coefficient In Plane 90°	µm/m.°C	9.06
	Thermal Expansion Coefficient Out of Plane	µm/m.°C	75.58
DMA*	Storage Modulus	GPa	12.8 ± 2.87
	Tan Delta Peak	°C	125.1 ± 1.69
Thermal Diffusivity	Thermal Diffusivity (at 25°C)	mm^2/s	0.436 ± 0.007
	Thermal Conductivity (at 25°C)	W/(m.K)	0.582 ± 0.009

* Thermal expansion coefficient and storage modulus values were given for the range below glass transition temperature.

APPENDIX C

MECHANICAL TESTING OF PPS/CF SPECIMENS

It is known that mechanical testing of the composite laminates requires rather thicker and proper specimen production. Therefore, in this thesis, PPS/CF laminates were also consolidated by using "autoclave molding" technique. The advantage of autoclave molding is apart from precise temperature and pressure control; vacuum action could be also applied so that it is possible to produce high-quality thermoplastic composite laminates with rather lower void content.

For this purpose, first prepregs were cut into 250 mm x 265 mm by the aid of an automated ply cutter. Then, in order to get 3 mm thick laminates 10 plies were laid down onto a rectangular tool. After detailed proper "plastic bagging" and "vacuum sealing" stages, the assembly was placed into the autoclave chamber (*Sistem Teknik*) as shown in Figure C.1 (d). Then, certain sequences of the pressuring, vacuuming, heating and curing steps tabulated in Table C.1 were applied.

Table C.1 Steps used during laminate consolidation by autoclave molding.

|	
Step 1	Apply vacuum at 760 mmHg
Step 2	Increase pressure up to 2.0 bar
Step 3	Increase temperature up to 315°C with 5°C/min ramp
Step 4	Increase pressure up to 8.0 bar
Step 5	Wait for 15 min at 315°C
Step 6	Cool down to 160°C with 5°C/min ramp
Step 7	Reduce pressure down to 4.0 bar
Step 8	Cool down to RT with 5°C/min ramp
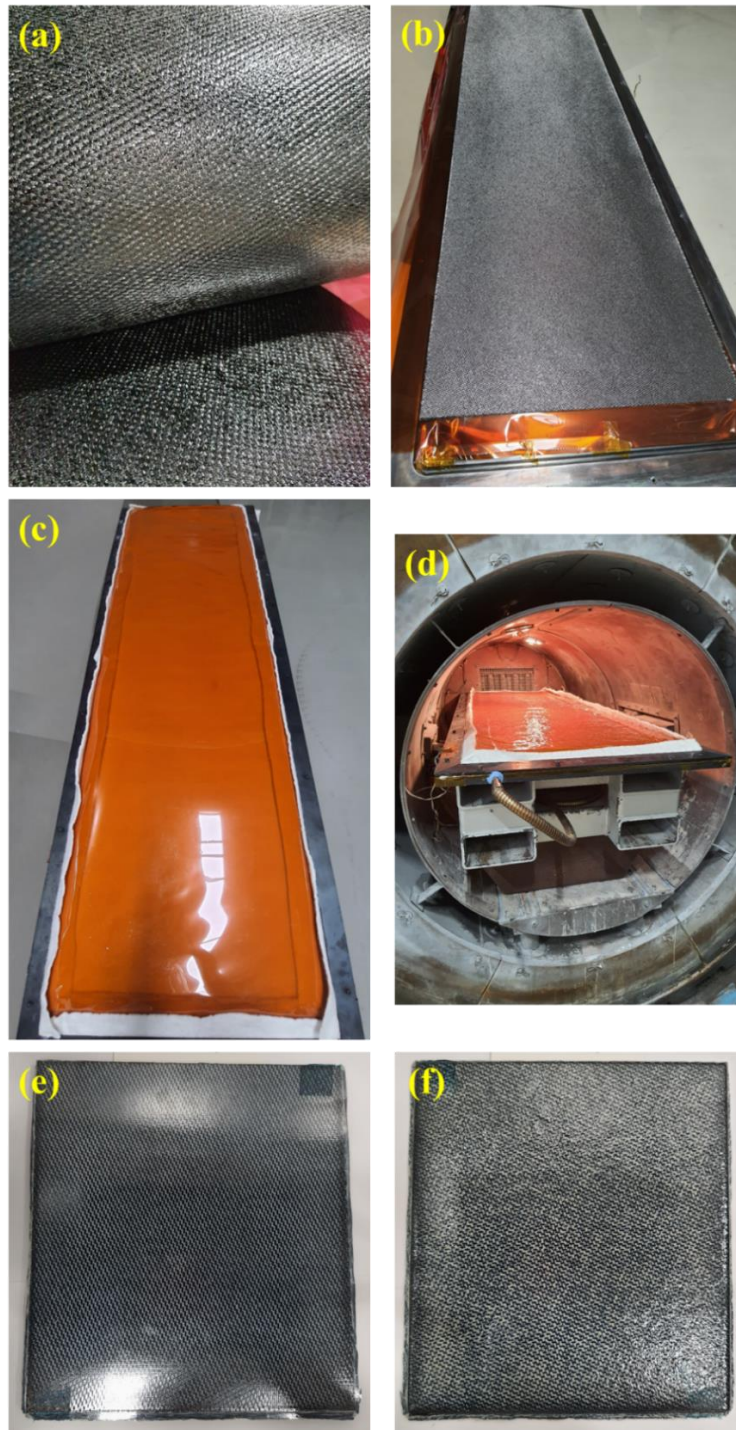
Figure C.1 Production of the PPS/CF laminates by Autoclave Molding for mechanical tests: (a) and (b) Prepreg lay-up, (c) Plastic bagging, (d) Consolidation by autoclave molding, (e) Mold side surface, and (f) Plastic bagging side surface of the laminate produced.

Mechanical properties of PPS/CF specimens were determined in two groups of tests: (i) Bulk properties, i.e. Strength and Modulus, under three different loadings of Tensile, Compressive, and Flexural; and (ii) Interlaminar Properties, i.e. Shear Strength and Fracture Toughness. For the first group a Universal Testing System of 250 kN capacity (*Instron 5985*), while for the second group a system with 10 kN capacity (*Instron 68TM*) were used.

Tensile, Compressive and Flexural Tests:

Tensile Strength and Modulus values of the specimens (2 x 25 x 250 mm) were determined in accordance to ISO 527-4 standard (Figure C.2 (a)); while Compressive Strength and Modulus values of the specimens (2 x 25 x 150 mm) were determined in accordance to ASTM D3410 standard (Figure C.2 (b)). During tensile and compressive tests, measurements were done along both longitudinal and transverse directions, with proper specimen tabbing. In order to determine Flexural Strength and Modulus values of the specimens (3 x 10 x 130 mm), Three- Point Bending tests were conducted in accordance to ASTM D7264 standard (Figure C.2 (c)).

Short-Beam Strength and Fracture Toughness Tests:

Interlaminar Shear Strength values of the specimens (3 x 6 x 18 mm) were determined via Short-Beam Strength tests according to ASTM D2344 standard (Figure C.2 (d)). Interlaminar Fracture Toughness Energy values of the specimens were obtained under two different loading; Mode-I (opening mode) and Mode-II (sliding mode) in accordance to EN6033 and EN6034 standards, respectively (Figure C.2 (e) and (f)). Pre-cracks required in these two tests were formed by consolidating a release film in between the two 1.5 mm thick laminate specimens.

Examples of the load-displacement curves obtained from these Mechanical Tests are given in Figure C.3, while the mechanical properties determined are tabulated in Table C.2.
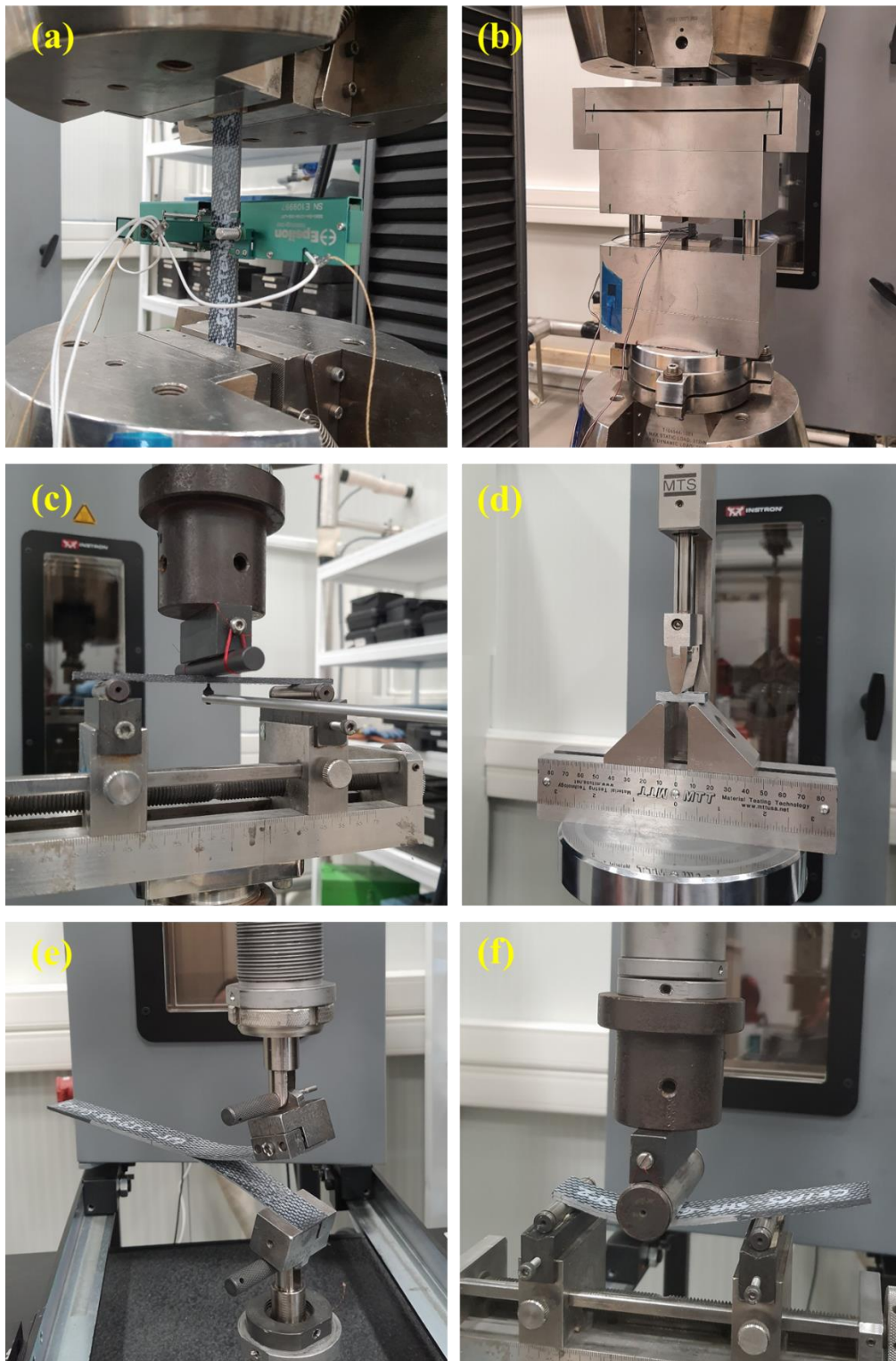
Figure C.2 Mechanical testing of PPS/CF specimens: (a) Tensile, (b) Compressive, (c) Flexural, (d) Short-Beam Strength, (e) and (f) Fracture Toughness under Mode-I and Mode-II.
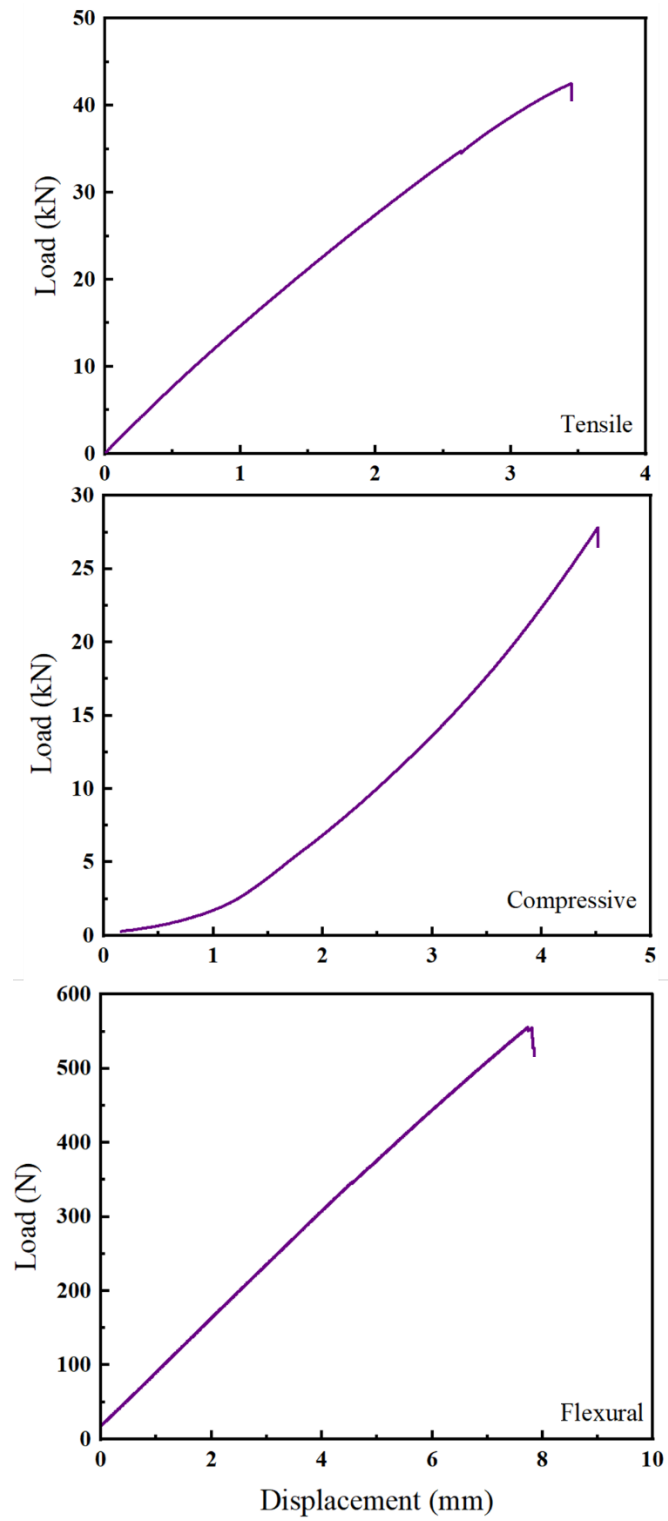
Figure C.3 Examples of the load-displacement curves obtained during mechanical testing of PPS/CF specimens: (a) Tensile, (b) Compressive, (c) Flexural, (d) Short-Beam Strength, (e) and (f) Fracture Toughness under Mode-I and Mode-II.

81
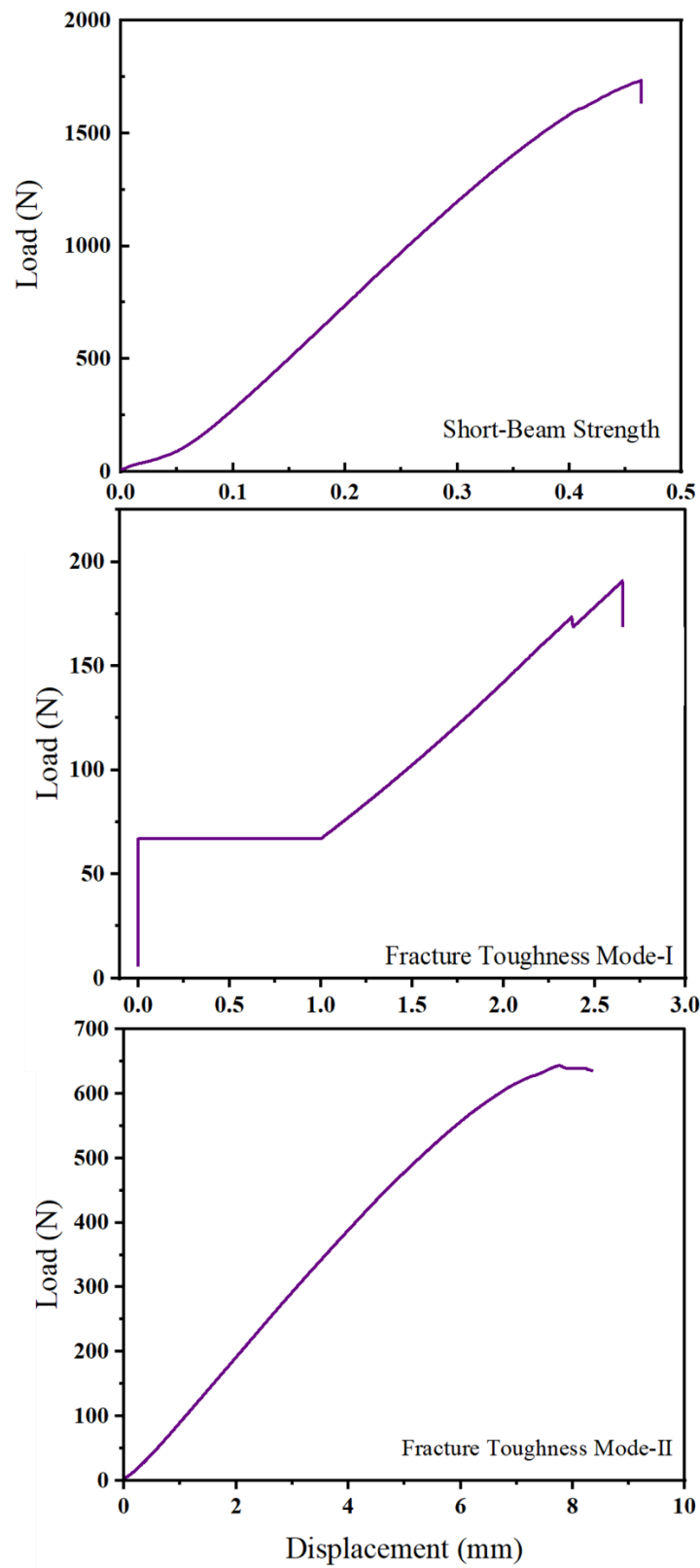
Figure C.3 (Continued.)

Table C.2 Mechanical properties of PPS/CF specimens determined from mechanical tests.

Property	Unit	Value
Tensile Strength 0°	MPa	792 ± 55.0
Tensile Strength 90°	MPa	720 ± 45.3
Tensile Modulus 0°	GPa	55.6 ± 1.61
Tensile Modulus 90°	GPa	56.6 ± 0.99
Compressive Strength 0°	MPa	533 ± 27.2
Compressive Strength 90°	MPa	532 ± 23.7
Compressive Modulus 0°	GPa	63.5 ± 3.40
Compressive Modulus 90°	GPa	55.7 ± 1.02
Flexural Strength	MPa	763 ± 10.5
Flexural Modulus	GPa	51.1 ± 0.85
Short-Beam Strength	MPa	70.5 ± 2.32
Fracture Toughness Mode-I	kJ/m^2	1.01 ± 0.01
Fracture Toughness Mode-II	kJ/m^2	2.28 ± 0.08

APPENDIX D

LASER AND PLASMA TREATMENT PARAMETER TRIALS AND THEIR CONTACT ANGLE-SURFACE ENERGY VALUES

Table D.1 Laser treatment parameters used during 12 trials, and the average values of Water Contact Angles (θ) measured, together with total Surface Free Energy (γ_{SV}) and their estimated values of Dispersion (γ_{SV}^{D}), Polar (γ_{SV}^{P}) Components of the PPS/CF samples.

	Laser Treatment Parameters Used				θ	γ_{SV}^{D}	γ_{SV}^{P}	γ_{SV}
Trial #	Laser Power (mW)	Scanning Speed (mm/s)	Pulse Distance (µm)	Focal Distance (mm)	(°)	(mJ/m²)	(mJ/m²)	(mJ/m²)
1	100	30	100	11	67.95	26.63	12.90	39.53
2	100	40	100	11	69.06	26.63	12.25	38.88
3	100	50	100	11	74.41	27.59	8.92	36.52
4	100	30	200	11	66.75	25.50	14.16	39.66
5	100	40	200	11	69.29	26.67	12.10	38.77
6	100	50	200	11	73.99	26.50	9.56	36.07

Table D.1 (Continued.)

7	140	30	100	11	62.61	29.07	14.97	44.04
8	140	40	100	11	65.31	26.23	14.69	40.92
9	140	50	100	11	67.96	26.35	13.02	39.38
10	140	30	200	11	66.79	29.68	12.22	41.91
11	140	40	200	11	69.86	27.24	11.52	38.76
12	140	50	200	11	68.84	22.57	14.36	36.93
13	170	30	100	11	69.37	27.36	11.75	39.11
14	170	40	100	11	65.86	26.70	14.12	40.82
15	170	50	100	11	66.06	24.74	14.98	39.72
16	200	30	100	11	70.98	26.93	11.02	37.95
17	200	40	100	11	66.35	24.72	14.80	39.52
18	200	50	100	11	66.11	24.05	15.30	39.35
19	230	30	100	11	65.91	29.80	12.68	42.48
20	230	40	100	11	63.97	26.13	15.58	41.71
21	230	50	100	11	63.55	27.46	15.18	42.64
22	170	30	200	11	72.53	32.61	8.09	40.70
23	170	40	200	11	71.26	33.16	8.53	41.68
24	170	50	200	11	69.21	33.78	9.34	43.12
25	170	30	100	10	66.50	31.03	11.83	42.86
26	170	40	100	10	57.55	30.31	17.50	47.82
27	170	50	100	10	55.12	30.03	19.20	49.22

28	170	30	100	9	57.24	32.89	16.45	49.34
29	170	40	100	9	55.43	30.60	18.70	49.30
30	170	50	100	9	58.62	30.86	16.57	47.43
31	170	30	200	10	67.01	29.46	12.19	41.66
32	170	40	200	10	66.45	27.66	13.31	40.98
33	170	50	200	10	67.70	28.78	12.09	40.87
34	170	30	200	9	62.68	29.95	14.52	44.47
35	170	40	200	9	67.65	31.36	11.06	42.42
36	170	50	200	9	69.07	26.68	12.22	38.90
37	100	30	100	9	67.62	31.12	11.17	42.29
38	100	40	100	9	66.93	31.57	11.37	42.95
39	100	50	100	9	65.00	28.90	13.62	42.52
40	140	30	100	9	55.2	30.18	19.06	49.24
41	140	40	100	9	57.43	29.03	18.24	47.27
42	140	50	100	9	59.49	30.32	16.30	46.62
43	200	30	100	9	56.30	31.67	17.61	49.28
44	200	40	100	9	65.95	35.21	10.52	45.73
45	200	50	100	9	73.79	35.57	6.60	42.17
46	230	30	100	9	84.41	40.20	1.94	42.14
47	230	40	100	9	75.37	36.23	5.75	41.98
48	230	50	100	9	62.25	32.22	13.77	45.98

Table D.2 Plasma treatment parameters used during 12 trials, and the average values of Water Contact Angles (θ) measured, together with total Surface Free Energy (γ_{SV}) and their estimated values of Dispersion (γ_{SV}^D), Polar (γ_{SV}^P) Components of the PPS/CF samples.

	Plasma Treatment Parameters Used			θ (°)	γ_{SV}^D (mJ/m²)	γ_{SV}^P (mJ/m²)	γ_{SV} (mJ/m²)
Parameter Trial #	Scanning Speed (mm/s)	Nozzle to Surface Distance (mm)					
1	5	6		15.93	35.49	36.61	72.10
2	20	6		23.33	35.87	33.74	69.61
3	100	6		28.57	35.63	31.57	67.19
4	150	6		27.72	34.62	32.61	67.23
5	5	12		19.22	35.46	35.57	71.03
6	20	12		27.71	36.36	31.52	67.88
7	100	12		24.45	35.23	33.68	68.92
8	150	12		26.74	35.54	32.48	68.02
9	5	24		18.83	35.63	35.59	71.22
10	20	24		25.07	36.13	32.84	68.97
11	100	24		41.83	37.13	23.60	60.73
12	150	24		49.63	39.53	17.92	57.45